Research Square

Preprints are preliminary reports that have not undergone peer review.
They should not be considered conclusive, used to inform clinical practice,
or referenced by the media as validated information.

Viscereality: Bioresponsive Virtual Reality for Box Breathing and Altered-State Experience

George Fejer

fejer@mpib-berlin.mpg.de

Max Planck Institute for Human Development

Till Holzapfel

University of Duisburg-Essen

Taru Hirvonen

Anestis Lalidis Mateo

Hochschule Bielefeld

Johannes Blum

Pädagogische Hochschule Schaffhausen

Michael Gaebler

Max Planck Institute for Human Cognitive and Brain Sciences

Bigna Lenggenhager

AIR—Association for Independent Research

Research Article

Keywords: biofeedback, breath-based interaction, breathwork, altered states of consciousness, particle systems

Posted Date: September 11th, 2026

DOI: https://doi.org/10.21203/rs.3.rs-10842634/v1

License: This work is licensed under a Creative Commons Attribution 4.0 International License.
Read Full License

Additional Declarations: No competing interests reported.

Viscereality: Bioresponsive Virtual Reality for Box Breathing and Altered-State Experience

George Fejer[1,2,3,4*], Till Holzapfel[5], Taru Hirvonen, Anestis Lalidis Mateo[7], Johannes Blum[6], Michael Gaebler[1,2], Bigna Lenggenhager[8,9]

[1*]Max Planck Institute for Human Development, Berlin, Germany.
[2]Max Planck Institute for Human Cognitive and Brain Sciences, Leipzig, Germany.
[3]University of Konstanz, Konstanz, Germany.
[4]ALIUS Research Network, Berlin, Germany.
[5]University of Duisburg-Essen, Research Center Trustworthy Data Science and Security, Duisburg, Germany.
[6]Pädagogische Hochschule Schaffhausen, Schaffhausen, Switzerland.
[7]Institute for Building Intelligence, Hochschule Bielefeld - University of Applied Sciences and Arts, Bielefeld, Germany.
[8]AIR—Association for Independent Research, Zurich, Switzerland.
[9]Department of Psychology, University of Zurich, Zurich, Switzerland.

*Corresponding author(s). E-mail(s): george.fejer@aliusresearch.org;
Contributing authors: tillholzapfel@gmail.com; 2taruhi@gmail.com; alalidis@hsbi.de; johannes.blum@phsh.ch; gaebler@mpib-berlin.mpg.de; bigna.lenggenhager@gmail.com;

Abstract

Breath-based interactions in virtual reality typically map breathing onto discrete visual objects or physiological proxies. Viscereality instead translates respiratory state into a surrounding particle field, mapping lung volume onto external space so that inhalation expands the environment and exhalation contracts it. Because particle fields have no fixed boundary, they can convey information through the motion and interactions of many simple elements. We tested whether this virtual-reality paradigm could reliably elicit altered-state experiences during box breathing, whether transient symmetric particle coupling would further influence subjective experience, and whether participants could identify the manipulation.

In a preregistered within-subjects study, 39 participants completed three counterbalanced 10-minute audio-guided box-breathing sessions: a high-symmetry virtual-reality condition, an asymmetric virtual-reality condition, and a dark-screen control. We assessed breathing adherence, altered states of consciousness, pictographic self-related measures, and sensitivity to the symmetry manipulation. Relative to the dark-screen control, the pooled virtual-reality conditions improved breathing synchronization, increased ratings of the perceived spatial extension of the self, and produced altered-state profiles with strong Perceptual Effects, moderate Positive Effects, and weaker Distressing Effects. Participants detected some symmetry-relevant features above chance, but neither reliably identified which session was symmetric nor showed outcome differences between the two virtual-reality mappings. These findings show that the overall virtual-reality paradigm produced reliable experiential differences from the control, but they do not establish that bioresponsiveness rather than visual engagement caused those differences. The specific affective contribution of particle symmetry, and whether it requires explicit awareness, therefore remain unresolved.

Keywords: biofeedback, breath-based interaction, breathwork, altered states of consciousness, particle systems

1 Introduction

Breathing is unique among visceral processes in that it is both automatically regulated and voluntarily controllable (Corne and Bshouty 2005; Baertsch et al. 2025). Respiratory patterns covary with affect. Arousing negative states have been associated with faster, shallower breathing, whereas relaxation has been associated with slower, deeper patterns (Boiten et al. 1994; Homma and Masaoka 2008; Jerath and Beveridge 2020). Voluntary changes in breathing can in turn modulate arousal and emotional state (Ashhad et al. 2022; Jerath and Beveridge 2020). This bidirectionality underlies breathwork (Fincham et al. 2023), which ranges from slow-paced exercises used for relaxation and emotional regulation (Zaccaro et al. 2018; Bentley et al. 2023) to high-ventilation techniques that can evoke pronounced bodily and perceptual changes, sometimes accompanied by emotional catharsis (Bahi et al. 2024; Havenith et al. 2025; Fincham et al. 2026; Schmitz et al. 2026).

The capacity to regulate arousal and affect through respiration has motivated applications of respiratory biofeedback in VR, including meditation (Tinga et al. 2019), anxiety and stress regulation (Bossenbroek et al. 2020; Blum et al. 2019), and respiratory rehabilitation (Shi et al. 2023). More broadly, breath-based interaction treats respiration as an experiential modality for VR design, in which visualisations extend awareness of an ongoing bodily process by rendering it perceptible and can thereby shape both task performance and the quality of experience during breathing exercises (Prpa et al. 2020). In respiratory VR, the term exteroceptive–interoceptive sensory

George Fejer and Till Holzapfel contributed equally and share first authorship. Taru Hirvonen and Anestis Lalidis Mateo contributed equally and share second authorship. Johannes Blum is the third author. Michael Gaebler and Bigna Lenggenhager share senior authorship.

substitution has been used to describe this design principle, whereby an internal respiratory signal is translated into an external sensory event that remains experientially linked to the body (Goral et al. 2024). How that signal is given spatial form is therefore a central design question.

Prior breath-based VR work has mapped respiration onto discrete targets or virtual bodies (Tinga et al. 2019; Monti et al. 2020; Wald et al. 2023), used it to drive locomotion (Bossenbroek et al. 2020; Rockstroh et al. 2021), or coupled it to local scene changes (Blum et al. 2020). Across these systems, breathing controls a target or scene parameter rather than the extent of surrounding space (Tinga et al. 2019; Monti et al. 2020; Bossenbroek et al. 2020; Rockstroh et al. 2021; Blum et al. 2020; Wald et al. 2023). Viscereality instead maps estimated lung volume onto an immersive particle field that expands away from the user during inhalation and contracts inward during exhalation (Fejer et al. 2025, 2026a). A short video summary is archived at https://osf.io/4enfg and is also available at https://www.youtube.com/watch?v=Qm-lmC-xYCI. The field renders this movement through the relative displacement of discrete elements, consistent with evidence that transformations of random-dot arrays can provide compelling cues to three-dimensional surface depth (Rogers and Graham 1979). Because this mapping provides continuous spatial feedback about respiratory phase and amplitude, it motivates the prediction that the bioresponsive VR conditions will improve adherence to the guided rhythm.

Other VR studies have used abstract forms with diffuse boundaries to elicit altered states (Glowacki et al. 2020, 2022; Vidal et al. 2025). Glowacki describes this as a weakly representational aesthetic, in which forms remain perceptually coherent without depicting fixed, familiar objects (Glowacki 2024). Viscereality shares this principle because its particle field forms a flexible spatial medium rather than a set of discrete virtual objects.

The spatial mapping also motivates a self-related hypothesis. Cardiac-synchronous visual feedback has altered self-location in a full-body paradigm (Aspell et al. 2013) and body ownership in a rubber-hand paradigm (Suzuki et al. 2013). Respiratory-synchronous feedback has enhanced body ownership when mapped to a virtual body (Monti et al. 2020) and agency when mapped to a focal object (Wald et al. 2023). Peripersonal space, the multisensory region surrounding the body, is malleable and contributes to the represented boundary between self and environment (Bufacchi and Iannetti 2018; Serino 2019). In these paradigms, the manipulated feedback is attached to a body representation or focal object (Aspell et al. 2013; Suzuki et al. 2013; Monti et al. 2020; Wald et al. 2023). Viscereality instead couples breathing to the spatial extent of the environment (Fejer et al. 2025, 2026a). This may affect how far the self is experienced as extending into surrounding space. We therefore assess body-boundary salience (Dambrun 2016), spatial frame of reference (Hanley and Garland 2019), and perceived self-size (Vidal et al. 2025) as three complementary preregistered outcomes.

Beyond this breath-responsive spatial mapping, the particle field has a second property relevant to the present experiment. Inhalation and exhalation are represented through radial expansion and contraction, whereas the field's radius remains stable during the two breath-hold phases. Rather than leaving these phases visually

static, the particles continue to oscillate, change colour, and vary in size. In the high-symmetry condition, oscillator coupling transiently synchronises the phases of these ongoing motion, chromatic, and size cycles, producing coherent geometric patterns. In the anti-symmetry condition, fixed negative coupling keeps the same dynamics visually irregular (Section 2.3.3). We therefore introduced dynamic symmetry as a separate within-VR factor to test whether aesthetic organisation during breath holds affects experience. Both active conditions share the visual scene, breath-coupled spatial motion, and audio, while only oscillator coupling differs. Visual symmetry has been associated with positive valence (Bertamini et al. 2013; Makin et al. 2012) and pleasantness (Pecchinenda et al. 2014), while movement synchrony has been associated with greater enjoyment (Vicary et al. 2017). More speculatively, the manipulation was also informed by the symmetry theory of valence, which proposes that symmetry in the formal structure of an experience corresponds to its pleasantness (Johnson 2023). We preregistered the prediction that high symmetry would produce more positively valenced experience and stronger self-related changes than the anti-symmetry mapping. Because the manipulation is brief and embedded in continuous motion, condition-identification performance provides a methodological check on whether participants perceived the intended contrast.

We investigate the VR augmentation of slow-paced 4–4–4–4 box breathing for several pragmatic reasons. Its four equal-duration phases provide a regular target for quantifying adherence and a straightforward temporal structure for mapping particle-field expansion and contraction. The clinical and popular literature promotes box breathing and related slow-breathing techniques as brief relaxation and stress-regulation exercises that improve heart rate variability (HRV) (Marchant et al. 2025; Zaccaro et al. 2018; Laborde et al. 2022), which gives the technique an established experiential baseline. Some slow-paced practices produce altered-state experiences, such as slow nasal Samavritti breathing (Zaccaro et al. 2022), but pronounced alterations in subjective experience characterise high-ventilation breathwork (Bahi et al. 2024; Havenith et al. 2025; Fincham et al. 2026; Schmitz et al. 2026). High-ventilation breathwork carries its own risks in immersive VR when introduced to participants recruited from a general university pool. Contracting virtual environments can elicit involuntary defensive responses (Kodithuwakku Arachchige et al. 2022). Rapid motion in depth can also increase vection and VR discomfort (Pöhlmann et al. 2021). Slow-paced breathing does not typically produce pronounced shifts in conscious experience. This gives us a stable baseline for assessing whether the VR augmentation modulates altered-state experience against the psychometric standards the field uses to compare induction techniques (Studerus et al. 2010; Dittrich 1998).

We evaluate Viscereality in a preregistered within-subjects design (Section 2.5). The 39 included participants completed counterbalanced 10-minute box-breathing sessions in high-symmetry VR, anti-symmetry VR, and a dark-screen control (Sections 2.1 and 2.2). The pooled active-VR-versus-control contrast evaluates the overall immersive paradigm and does not isolate bioresponsiveness from visual engagement, whereas the within-VR contrast isolates the oscillator-coupling manipulation.

We assess breathing adherence, three pictographic measures of self-related experience, and altered-state experience (Section 2.4). We separately assess awareness of the symmetry manipulation (Section 2.4.4).

We predicted that the two Viscereality conditions, relative to the dark-screen control, would improve adherence to the guided box-breathing rhythm and alter subjective experience assessed by the preregistered 11D-ASC and self-related measures. Within the altered-state family, the preregistered directional ordering was high-symmetry VR > anti-symmetry VR > dark-screen control for Experience of Unity, Blissful State, and Audio-Visual Synesthesia (Section 2.5). Within VR, we also expected high symmetry to produce closer adherence to the guided rhythm and stronger self-related changes than the anti-symmetry mapping, although no separate direction was specified for each pictographic outcome. Condition-identification performance was treated as a methodological check rather than as an additional substantive hypothesis.

2 Methods

2.1 Participants

Participants were recruited from the University of Konstanz psychology student participant pool and received course credit for participation. The study used a within-subject design in which each participant completed all three conditions in one of six counterbalanced block-order permutations, with a preregistered target of 6 completers per permutation and 36 total. We did not systematically assess prior experience with virtual reality, meditation, breathwork, or psychedelics. We use recruitment-naive to mean that participants came from the general psychology participant pool through an advertisement for a VR breathing-biofeedback study rather than an altered-state or experience-seeking recruitment channel; it does not mean that prior experience was screened or absent. We tested 47 participants; 8 were excluded based on breathing signal quality (phase-locking value (PLV) outlier criterion described below), yielding a final sample of $N = 39$ (6–7 per permutation), preserving approximately equal representation across all six condition sequences. Among the included participants, mean age was 20.8 years; 37 were female (mean age 20.7 years) and 2 were male (mean age 23.0 years).

2.2 Design, Conditions, and Procedure

Participants were seated in a bean bag, wore noise-blocking headphones, held a controller against their abdomen, and completed all breathing blocks, questionnaires, and outcome measures fully immersed in virtual reality. The three-session procedure was automated end-to-end in the headset: once the headset was put on, participants followed in-VR instructions for the breathing blocks and all post-block outcome measures while remaining seated, with minimal experimenter intervention beyond initial setup and debriefing. Before the experimental sequence, participants completed a 1-minute guided breathing practice block for acclimation, familiarizing them with controller placement and the paced-breathing rhythm. Each participant then completed three conditions, with session order assigned automatically by random selection from

the six counterbalanced block-order permutations. Because the dynamic symmetry manipulation was embedded in the software-controlled scene logic and the condition sequence was assigned automatically at runtime, neither the participant nor the experimenter knew which condition would appear in which session. In all conditions, participants followed a 10-minute audio-guided box-breathing exercise (sourced from a publicly available recording) consisting of repeated 4-4-4-4 cycles with four seconds each of inhalation, breath hold, exhalation, and breath hold. In the high-symmetry condition, the bioresponsive particle environment formed dynamic symmetric patterns during breath-hold phases. In the asymmetric condition, visual features of the particles remained asymmetric to one another throughout. In the dark-screen control condition, the particle environment was not displayed; participants viewed a dark field containing only a central fixation marker that also provided breathing-performance feedback (Section 2.3.4). We refer to this condition as the "dark-screen control" throughout. After each block, participants completed the full assessment battery (questionnaires and pictographic scales) while remaining in virtual reality. Figure 1 summarizes the full procedure, including the repeated condition loop and blinding sequence, using the same condition-color mapping as the Results figures.

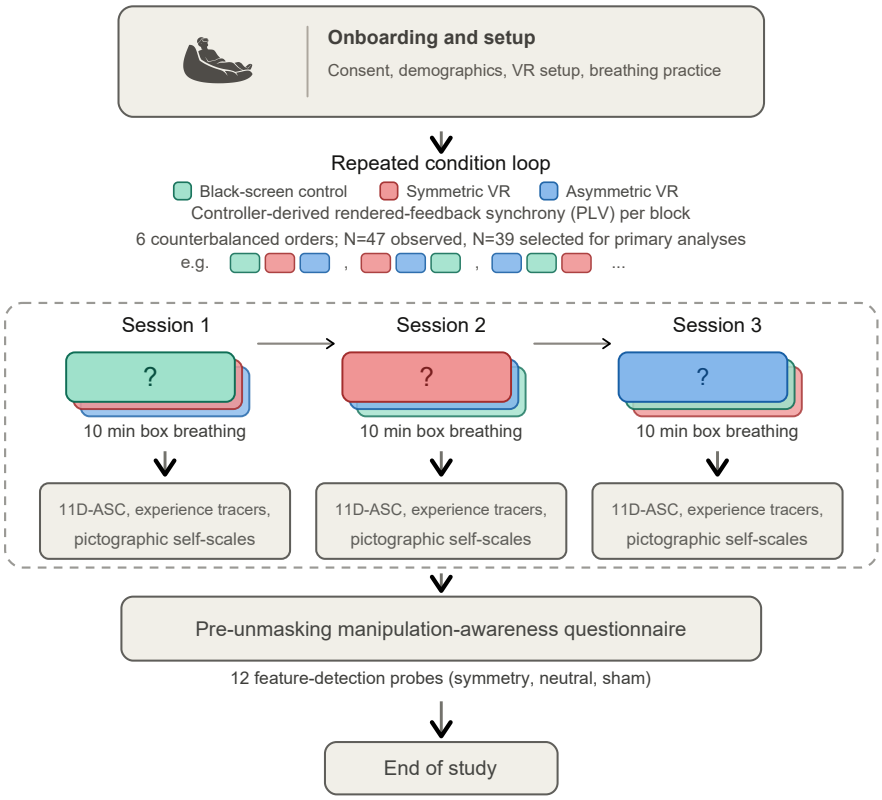


Fig. 1 Study procedure. After onboarding, each participant completed three 10-minute box-breathing sessions (dark-screen control, symmetric VR, asymmetric VR) in one of six counterbalanced orders, with the full assessment battery administered in VR after each block. A blinding questionnaire followed the third block before the study concluded

2.3 Virtual-Reality Intervention

Viscereality is a bioresponsive virtual-reality system that maps respiratory signals to dynamic visual feedback within an immersive 3D particle environment (Fejer et al. 2025, 2026a). The system runs on a Meta Quest 3 headset (standalone, untethered) and was built in Unity, with CPU-optimized parallel processing (Unity Job System with Burst compilation) maintaining a stable 72 Hz frame rate. The two active virtual-reality conditions used the same visual environment, audio guidance, and logging pipeline; they differed only in a single engine parameter controlling oscillator coupling dynamics. The dark-screen control used identical audio guidance and data logging but omitted the particle visualization. We focus here on the experiment-relevant functional logic; fuller technical and implementation details of the Viscereality engine are described in the prior system papers (Fejer et al. 2025, 2026a).

2.3.1 Breath Detection

Breath detection follows the approach introduced by Flowborne (Rockstroh et al. 2021), using the VR controller's positional tracking to infer respiratory displacement without additional sensors. During an initial calibration, the user places the controller against the lower abdomen to establish a tracking axis. Each frame, the algorithm reads the controller's position and orientation, projects motion onto this breathing-relevant axis, and updates a short-term versus long-term smoothed motion estimate. The difference between these smoothed signals functions as a breathing trend signal. Positive values indicate inhalation, negative values indicate exhalation, and near-zero values indicate a pause. Samples are rejected as tracking artifacts if controller rotation is too abrupt or if the inferred trend is implausibly large. The resulting classification (inhale, exhale, pause, or bad tracking) drives the visual feedback pipeline described below (Figure 2). Detailed implementation choices and parameterization are documented in the Viscereality technical descriptions (Fejer et al. 2025, 2026a).

2.3.2 Sphere Radius and Visual Feedback

The user is positioned at the center of a large particle-covered sphere. The primary feedback loop couples sphere radius to breathing. Inhalation causes the sphere to expand outward, exhalation causes it to contract inward, and breath holds maintain the current radius. Functionally, the controller-derived breathing-state label is converted into a signed expansion/contraction command whose magnitude is scaled to the configured radius range and the intended inhale/exhale timing. That command updates a target sphere radius, and the rendered radius is then smoothed with a damped interpolation step (0.25 s smooth time; overshoot prevention enabled). In practice, this means participants do not see a raw controller-motion trace; they see a bounded, temporally stable visual signal that preserves breathing direction while suppressing jitter. Full implementation details of the radius controller are described in the prior Viscereality system reports (Fejer et al. 2025, 2026a).

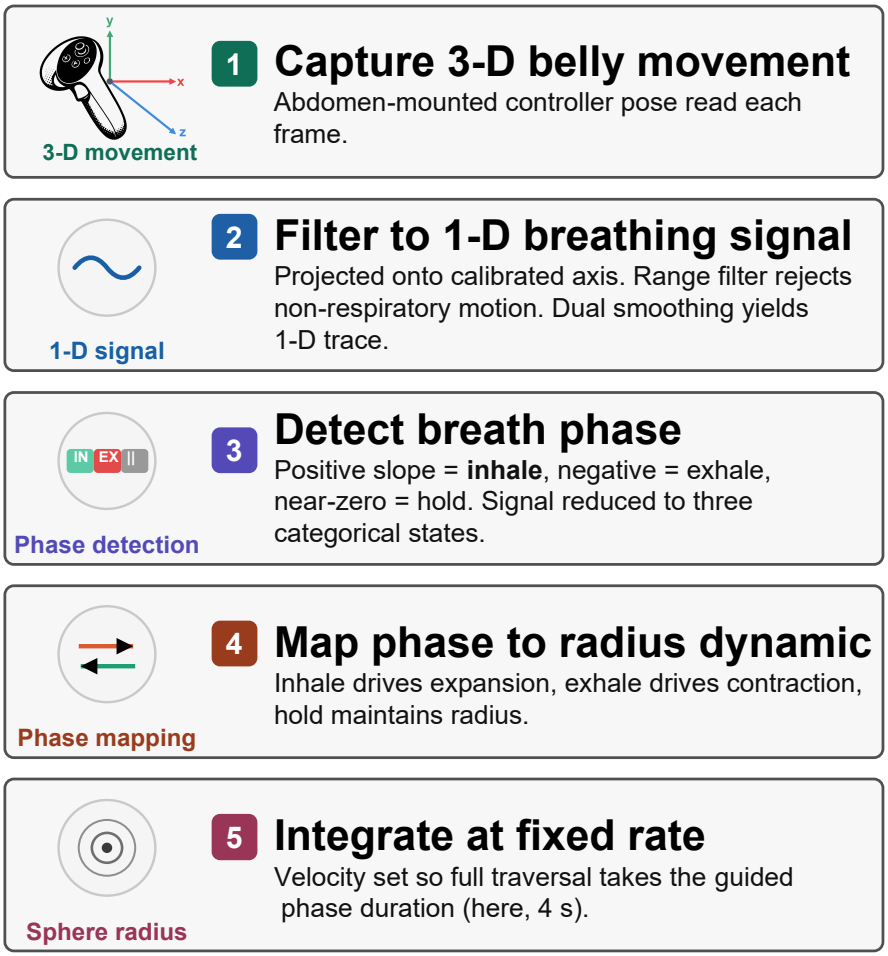


Fig. 2 Signal processing pipeline from abdomen-mounted controller motion to rendered sphere radius. Raw 3D movement is projected onto a calibrated breathing axis, classified into inhale, exhale, or hold phases, and mapped onto expansion and contraction dynamics that update the visible sphere at a fixed velocity

The sphere surface is composed of approximately 2,500 view-aligned ring particles distributed on an icosphere mesh for uniform geodesic spacing. Each particle is rendered with a radial gradient that produces depth cues through overlap, and during expansion and contraction, particles generate cone-like tracer effects that reinforce the perception of three-dimensional movement. Surface wave oscillations, structured noise, and unsynchronized chromatic cycles maintain continuous visual dynamics across all breathing phases, preventing the environment from appearing static during breath holds (Fejer et al. 2025).

2.3.3 Oscillator Network and Condition Manipulation

The second layer of the system implements a Kuramoto oscillator network across the sphere's vertices (Acebrón et al. 2005; Rodrigues et al. 2016). Each particle has an internal oscillation phase (analogous to a clock angle) and interacts with its neighbors through coupling weights that determine whether nearby particles tend toward synchronization or away from it. If the coupling weight is positive, neighbors are pulled toward shared timing (phase attraction). If negative, the interaction becomes *anti-coupling*, and neighbors are pushed away from alignment (phase repulsion).

The network uses a two-tier neighbor structure reflecting the icosphere topology. Most vertices have 6 immediate (tier-1) neighbors and 12 next-nearest (tier-2) neighbors, while 12 vertices at the original icosahedron poles have 5 tier-1 neighbors. At each update step, each oscillator advances according to its own intrinsic rhythm plus a neighborhood interaction term. In plain terms, the algorithm compares an oscillator's current phase with those of its neighbors and then adjusts it toward or away from them depending on the sign and magnitude of the tier-specific coupling weights. This is the standard Kuramoto logic (phase-offset-dependent attraction/repulsion), implemented here with two neighbor tiers and a global coupling gain, and updated in parallel each frame together with particle position, size, and color. The underlying icosphere topology and two-tier Kuramoto architecture are described in the original Viscereality system paper (Fejer et al. 2025).

The two active conditions differed in how coupling weights were assigned. In the high-symmetry condition, tier-1 and tier-2 coupling weights were interpolated dynamically as a function of a coherence scalar (0–1), together with a coherence-dependent frequency scaling term. Verbally, low coherence pushes the system toward anti-coupled, irregular dynamics, whereas higher coherence progressively shifts interactions toward phase attraction and more synchronized motion. As a result, particle motion, color, and size periodically coordinate into coherent geometric patterns, such as flower-of-life-like lattices, during breath-hold phases before dissolving back into disorder when breathing resumes.

In the asymmetric condition, the system did not use this dynamic interpolation. Instead, coupling weights were held at fixed negative values (anti-coupling), so local interactions were permanently biased toward phase repulsion and the particle field remained visually irregular throughout. The manipulation was thus dynamical rather than geometric. The same scene, particles, and audio were used in both conditions, and only the oscillator interaction rules changed.

2.3.4 Breathing Performance Indicator

All three conditions displayed a minimal breathing performance indicator at the center of the participant's field of view. This consisted of a white pentagon ring whose individual line segments scaled with sphere radius: at half-volume (midpoint between full inhale and full exhale), the pentagon was fully visible; as the participant inhaled or exhaled toward the extremes, the segments progressively shortened and disappeared entirely at maximum and minimum volume. The indicator thus functioned as an unobtrusive loading-bar-style monitor of breathing excursion. Participants were instructed

that the goal was to make the pentagon disappear completely on each inhalation and exhalation, confirming sufficient breathing depth.

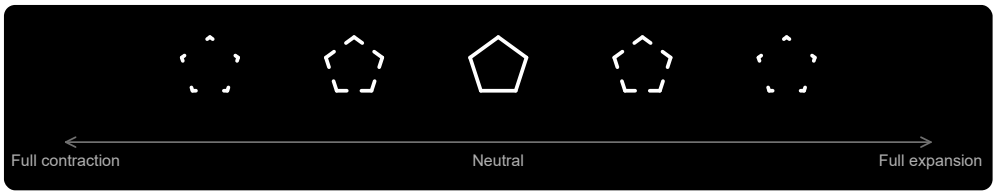


Fig. 3 Central breathing-performance indicator shown in all three conditions. The pentagon ring was fully visible at the neutral sphere radius and progressively disappeared toward full contraction or full expansion, providing condition-matched feedback about breathing excursion

2.4 Outcome Measures

We retained the five preregistered measurement blocks used in the assessment battery, but organize them here into four recurring outcome families that also structure the Results section. These were adherence to box breathing, self-related measures, altered states of consciousness, and the blinding questionnaire. Within the altered-states family, the main text presents the derived 3D-ASCr composites as a dimensionality-reduced summary; Online Resource 1, Section S3 reports the complete preregistered 11D-ASC analyses.

2.4.1 Adherence to Box Breathing

Adherence quantifies how closely each participant's breathing followed the instructed 4-4-4-4 box-breathing rhythm across each 10-minute block. The preregistered plan was to compute this from discrete phase labels produced by the breath-detection algorithm (Section 2.3.1), which classifies each frame as inhale, exhale, hold, or bad tracking. The intended metric was phase-duration error, defined as the absolute deviation from the 4-second target per breathing phase, averaged across valid cycles per condition, with participant exclusion if fewer than 70% of cycles were valid or if mean error exceeded 2 standard deviations above the sample mean.

The recorded phase sequences did not yield the expected clean succession of 4-second phases. Rather than discrete blocks of inhale, hold, exhale, and hold, the recorded data consisted of highly fragmented segments interspersed with brief transitional or ambiguous intervals. Computing phase-duration error from this data required first reconstructing plausible box-breathing cycles from the raw phase stream, a step that was not anticipated at preregistration. We explored several reconstruction strategies, including rule-based merging of adjacent micro-segments and temporal smoothing algorithms, but each approach introduced its own arbitrary parameter choices, such as minimum segment duration thresholds, smoothing window widths, and rules for combining adjacent same-phase fragments, that could materially influence the resulting error estimates. Because these post-hoc binning decisions carried more researcher degrees of freedom than the original preregistered metric implied, we adopted an alternative approach.

We quantified adherence as the phase-locking value (PLV) between two continuous time series. One was the sphere-radius signal that participants actually saw as visual feedback during the breathing session. The other was an ideal reference radius trajectory derived from the audio-instruction timestamps for perfect 4-4-4-4 breathing. PLV measures how consistently the phase relationship between two signals remains stable over time. A value near 1 indicates that the participant's breathing closely tracked the instructed rhythm throughout the block. A value near 0 indicates little consistent alignment. This approach circumvents the phase-reconstruction problem entirely, because it evaluates alignment at the level of the continuous visual feedback signal rather than attempting to recover discrete phase boundaries from a fragmented controller trace. PLV thus captures the same underlying construct as the preregistered metric, namely how closely breathing tracked the instructed rhythm, while avoiding the measurement artifacts that any post-hoc phase-segmentation strategy would have introduced. Figure 4 illustrates the relationship between observed and reference trajectories for a representative participant; the fragmented phase-label structure visible in the lower bars of each panel motivates the PLV-based approach described above.

Because PLV does not decompose into per-cycle validity counts, the preregistered 70%-valid-cycle plus 2-SD mean-error exclusion rule could not be transferred directly. Outlier exclusion instead used a lower-tail global IQR rule on condition-level PLV values, elevated to participant-level exclusion if any condition was flagged. Online Resource 1, Section S2 describes PLV computation and quality screening in detail.

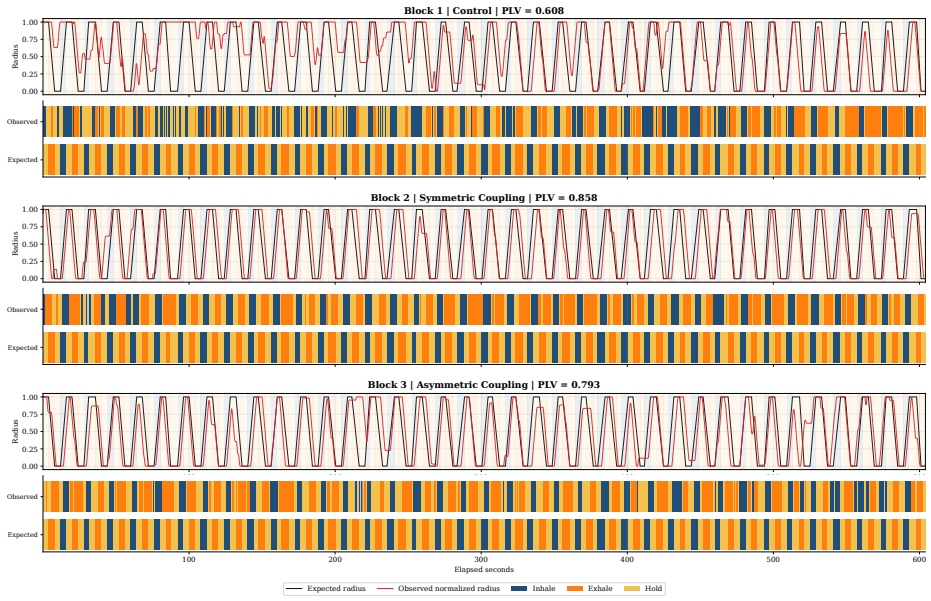


Fig. 4 Breathing dynamics for a representative participant (P01) across all three conditions. Observed sphere-radius traces (orange) are overlaid on the ideal 4-4-4-4 reference (blue), with per-block PLV values shown at right. Fragmented phase-label bars below each time series illustrate the segmentation noise that motivated the switch from phase-duration error to PLV as the adherence metric. Equivalent figures for all participants are provided in the OSF repository

2.4.2 Self-Related Measures

Three single-item pictographic measures assessed self-related experience after each condition. The adapted Perceived Body Boundaries item (Dambrun 2016) presents seven silhouettes progressing from diffuse (A) to sharply delineated (G). Responses were mapped from A–G to 1–7, so higher analyzed scores indicate stronger boundary salience. For construct-facing exploratory correlations, the item was reverse-scored so that higher values indicate greater boundary dissolution. The Spatial Frame of Reference Continuum (SFoRC; Hanley et al. 2020) depicts a figure in concentric spatial zones from body-centered to environment-encompassing, indexing the degree to which the spatial sense of self extended beyond the body. The Small Self pictographic item was adapted from Vidal et al. (2025), who presented it as an ad hoc item. We included it because Viscereality is organized around a spatial metaphor and the item represents self-related experience through the spatial size of the self relative to its surroundings. PBBS and Small Self use A–G responses mapped to 1–7, whereas SFoRC uses A–H responses mapped to 1–8. Each measure yields a single ordinal score per condition. We recreated all three pictographs as SVG graphics for VR presentation, using the previously published versions as visual references. The vector format allowed direct and flexible control over graded visual properties, including transparency, line width, dash spacing, relative figure size, and spatial extent, while enabling sharp rendering at headset resolution without the resolution loss associated with scaling raster images. We generated the SVG files in December 2025 with OpenAI Codex using GPT-5.2-Codex, based on author instructions and the cited published pictographs. The authors reviewed the resulting SVG files and take responsibility for the final stimuli. The OSF reproducibility package (https://osf.io/64mwk/) provides the recreated stimulus set, SVG source files, administered item keys, and study materials; Online Resource 1, Section S6 provides the corresponding reproducibility map.

2.4.3 Altered States of Consciousness

3D-ASCr composites. The revised 3D-ASCr higher-order factor model became available after preregistration. It provides a parsimonious contemporary summary of the same preregistered 11D-ASC responses by organizing them into Positive, Distressing, and Perceptual Effects. This level of aggregation matches our broad theoretical interest in positively versus negatively valenced experience, while retaining a perceptual dimension, and avoids overinterpreting lower-order dimensions for which no specific predictions were made. We therefore use the 3D-ASCr composites as the main-text summary. Online Resource 1, Section S3 reports complete analyses of all 11 preregistered 11D-ASC dimensions.

11D-ASC Questionnaire. We assessed altered states with the 11-Dimensional Altered States of Consciousness Rating Scale (11D-ASC; 42 items, 0–100 visual analogue scales), a validated lower-order factorization of the OAV/APZ framework (Studerus et al. 2010; Dittrich 1998; Hovmand et al. 2024; Prugger et al. 2022). The 11 subscales were Experience of Unity (EU), Spiritual Experience (SE), Blissful State (BS), Insightfulness (IS), Disembodiment (DIS), Impaired Control and Cognition

(ICC), Anxiety (ANX), Complex Imagery (CI), Elementary Imagery (EI), Audio-Visual Synesthesia (AVS), and Changed Meaning of Percepts (CMP). Participants completed one condition-specific rating after each block.

Temporal Experience Tracers (Exploratory). Temporal experience tracers provide psychometric time-series ratings of the same 11 experiential dimensions.

For each dimension, one prompt consolidated the constituent questionnaire items into a construct-level description. After each condition, participants retrospectively drew the 11 intensity curves on a world-space time-by-intensity surface using the VR controller. Controller position was projected onto the drawing plane, input was gated through a trigger hold, and points were emitted at constant spatial spacing regardless of hand speed. Each trace was reduced to peak intensity, representing the strongest reported moment, and area under the curve (AUC), representing intensity accumulated across reconstructed session time (Figure 5). We focused on these two summaries because no hypothesis required finer temporal features such as onset, timing, slope, or variability. We treat the tracer analyses as exploratory; Online Resource 1, Section S5 provides the complete implementation, data reduction, analyses, and results.

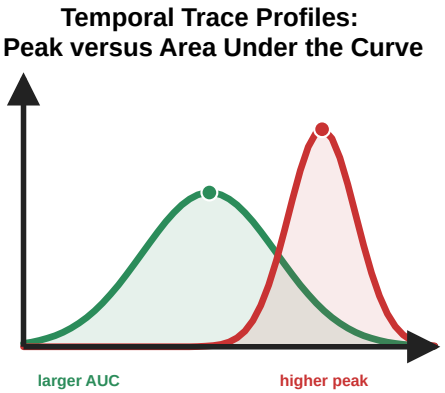


Fig. 5 Temporal experience tracers: peak and cumulative intensity. These hypothetical profiles illustrate information retained by psychometric time-series intensity ratings but not by a single retrospective visual-analogue-scale response. The red profile has a higher momentary peak, whereas the broader green profile has a larger area under the curve (AUC), reflecting greater cumulative intensity. Analyses in this paper focus on these two summaries because no hypothesis required finer-grained temporal features

2.4.4 Blinding Questionnaire

Blinding was assessed in two phases. In the pre-unmasking phase, participants were told that the study investigated how subtle differences in visual aesthetics might influence perception in virtual reality. We constructed a 12-item ad hoc masked-comparison questionnaire for this study. For each item, participants chose whether the feature was stronger in Scenario 1, stronger in Scenario 2, equal in both scenarios, or absent in both scenarios. The chance baseline was 0.25. Scenario labels referred to the two virtual-reality conditions in encounter order. The item set covered three hidden domains. These were manipulation-relevant symmetry/coordination cues that genuinely differed between the two VR conditions, matched comparison features that were present similarly in both conditions and therefore should be judged as equal, and foil (sham) features that were not present in either condition and therefore should be judged as absent. There were four items per domain.

In shorthand, the four symmetry-related items asked whether one scene more strongly showed transient coordination and ordering of the particle field, including particles moving as a coordinated group, becoming more organized or structured at certain moments, showing wave-like coordinated motion-and-color changes, or shifting from chaotic to ordered movement during breath holds. The four neutral matched

items asked about features that were present in both VR conditions to a similar degree, namely particles becoming brighter during breath holds, leaving faint motion trails during exhalation, remaining in gentle ongoing motion across the surface, or appearing to rise and fall like ocean waves. The four sham items were constructed as absent cross-modal or pulsing foils, asking about the music becoming quieter, the music seeming to slow down, particle motion and color changing in response to the music, or particles showing a size-based pulsing effect. To keep administration uniform while avoiding an obviously grouped structure, items from all three domains were intermixed in a single randomized order that was generated once in advance and then presented in that same order to all participants.

In the post-unmasking phase, participants were told that one condition featured brief visual synchronization during breath holds while the other remained irregular throughout. They indicated which session was more symmetric via a three-option forced choice (*first*, *second*, or *I don't know*), followed by a confidence rating.

2.5 Preregistration and Reproducibility

The study was preregistered on AsPredicted (#262,545). The unchanged registry record, all deidentified participant-level data, statistical analysis scripts and outputs, figure-generation scripts, and study materials were uploaded to OSF as a reproducibility package (https://doi.org/10.17605/OSF.IO/64MWK). We retained all preregistered design elements and outcome families. The preregistered analysis plan specified a repeated-measures ANOVA with condition as the within-subjects factor and presentation order as a covariate for each outcome, two planned contrasts (pooled VR versus dark-screen control, and symmetric versus asymmetric), and parallel Bayesian analyses. Adherence was to be quantified as phase-duration error with a cycle-validity exclusion rule, as described and motivated in Section 2.4.1. We deviated from this plan in several respects. Online Resource 1, Section S1 summarizes the deviations from preregistration and their rationale.

Adherence metric. Phase-duration error was replaced by PLV because the recorded phase-label data were too fragmented to yield reliable per-phase error estimates without introducing arbitrary binning decisions (see Section 2.4.1 for a full account). The associated exclusion rule was changed from 70%-valid-cycle plus 2-SD mean-error to a lower-tail global IQR rule on condition-level PLV values, because PLV does not decompose into per-cycle validity counts.

Omnibus condition test. For every non-PLV outcome, the preregistered order-adjusted repeated-measures analysis tests the condition effect after accounting for participant and numeric block position. It is implemented as a partial-F comparison between a participant-and-order model and the same model plus condition. Participant fixed effects provide within-participant blocking, and block position adjusts for presentation order. The finalized PLV omnibus remains unchanged. A condition-only repeated-measures ANOVA without the order covariate is retained in the OSF outputs as a sensitivity check.

Planned contrasts. The two preregistered planned contrasts were implemented as standalone paired t-tests, which yield the same paired contrast statistics as ANOVA

follow-ups in this within-subject setting. These serve as the confirmatory anchor for all multi-test outcome families in the Results section, and for significant planned contrasts in the altered-state families we additionally report paired common-language effect sizes (CLES), defined as the proportion of participants whose score was higher in the VR condition than in the dark-screen control (McGraw and Wong 1992).

Robustness and multiplicity. Because Shapiro–Wilk checks indicated non-normality for several condition-level and difference-score distributions, we added Wilcoxon signed-rank and Friedman tests as secondary distribution-free checks. The preregistration did not specify a multiplicity procedure. Nominal p values therefore govern the primary interpretation of the preregistered planned contrasts, with Benjamini–Hochberg q values reported as sensitivity information within the 11D-ASC, 3D-ASCr, and self-related outcome families. FDR-adjusted q values govern exploratory and post hoc screens. The OSF package contains the complete adjusted and distribution-free output; the paper reports material divergences from the primary planned-contrast interpretation.

3D-ASCr composites. The revised 3D-ASCr scoring scheme (Stocker et al. 2025) became available after preregistration. Because these composites are deterministic averages of the preregistered 11D-ASC subscale scores, they add no new participant data but do constitute a post-registration summary choice. We therefore use them to organize the main-text narrative while retaining the complete preregistered 11D-ASC analyses in Online Resource 1, Section S3.

Bayesian analyses. Bayesian analyses were preregistered and run in parallel on the same included sample ($N = 39$). Omnibus Bayes factors compared a point-null model without condition (H_0: outcome $\sim$ order + participant random intercept) against a model that additionally included condition (H_1: outcome $\sim$ condition + order + participant random intercept), using the BayesFactor R package with explicit prior settings (fixed-effect $r = 0.50$, continuous-covariate $r = \sqrt{2}/4 \approx 0.354$, random-effect nuisance $r = 1.00$; Morey and Rouder 2024; van Doorn et al. 2021; Kruschke 2021). For the two planned paired contrasts, we compared H_0 ($\delta = 0$) against two-sided H_1 ($\delta \neq 0$) using a Bayesian paired t-test with the default Cauchy prior on standardized effect size ($r = \sqrt{2}/2 \approx 0.707$; Morey and Rouder 2024; van Doorn et al. 2021). For EU, BS, and AVS, the preregistered joint ordering symmetric > asymmetric > dark-screen control was tested after block-position adjustment with an encompassing-prior Bayes factor against the equal-means null. Under the exchangeable condition-factor prior, each of the six strict condition orderings had prior probability 1/6. We report BF_{10} values (and $BF_{01} = 1/BF_{10}$ when the data favor the null) as relative evidence rather than as posterior probabilities or effect sizes (van Doorn et al. 2021; Kruschke 2021). Posterior median standardized effect sizes with 95% credible intervals and prior-robustness checks are reported in the OSF repository.

Blinding analyses. Pre-unmasking accuracy was scored using the documented answer key for the four symmetry, four neutral, and four sham items and across all 12 items. Mean accuracy was compared with the 0.25 chance baseline using Wilcoxon signed-rank tests, with Benjamini–Hochberg FDR correction across the four comparisons. Post-unmasking guesses were classified as correct (R), incorrect

(W), or uncertain (U) from the participant's selected active-VR session and condition order. The standard single-group Bang blinding index was calculated as BBI = $(R - W)/(R + W + U)$ (Bang et al. 2004; Kolahi et al. 2009), with a participant-bootstrap 95% confidence interval. Effective blinding was considered established only if the entire interval fell within $[-0.2, 0.2]$ (Qin et al. 2024; Kolahi et al. 2009). We also report an exploratory confidence-weighted directional index, calculated as the confidence-weighted proportion of correct directional guesses minus 0.5. The standard Bang interpretation bands were not applied to this modified index. To test whether pre-unmasking symmetry accuracy predicted subsequent condition identification, we calculated a point-biserial correlation between the 0–4 symmetry score and final-guess correctness, classified as correct versus incorrect or uncertain, with an exact two-sided permutation p value.

Exploratory analyses. We fit condition × PLV interaction models to test whether breathing synchronization moderated subjective effects. We also conducted an exploratory analysis of whether VR-related changes in the pictographic measures covaried with changes in ASC outcomes. For focused, construct-based interpretation, we examined SFoRC in relation to Experience of Unity and Disembodiment, including items concerning unity with the environment, floating, bodylessness, and altered self-location outside the body. We examined perceived body-boundary dissolution primarily in relation to Disembodiment and the same bodily-self items, and Small Self in relation to Experience of Unity, Spiritual Experience, and Blissful State. These thematic selections were post hoc and guided interpretation rather than defining separate inferential families. We additionally conducted broad exploratory screens across all 3D-ASCr composites, 11D-ASC subscales, and ASC items. Because only SFoRC showed a reliable pooled-VR-versus-dark-screen-control condition effect, the correlations were treated as exploratory tests of cross-measure correspondence rather than as evidence that all three pictographic measures changed under VR. Online Resource 1, Section S4 reports the complete analysis, with false-discovery-rate correction across all 9 composite, 33 subscale, and 126 item-level associations, together with symmetric-minus-asymmetric change correlations and order-adjusted participant-aware condition-interaction models.

3 Results

Across the four recurring outcome families, condition effects were consistently driven by the contrast between virtual-reality conditions and the dark-screen control. No outcome showed a reliable symmetric-versus-asymmetric difference. We report the results in the same family order used in Methods: adherence, self-related measures, altered states of consciousness, and the blinding questionnaire. For the non-PLV multi-test families, confirmatory interpretations are anchored in the preregistered planned contrasts evaluated as paired t-tests, with the registered order-adjusted participant-blocked partial-F omnibus noted for each family as context; PLV retains its finalized mixed-effects omnibus. Wilcoxon signed-rank robustness checks, Friedman omnibus tests, and FDR-adjusted q values are documented in the OSF repository and are mentioned here only when they materially qualify the paired t pattern.

3.1 Sample and Exclusions

The dataset contained records from all 47 tested participants. Condition-level PLV values from all participants were used to apply the quality-screening procedure described in Section 2.4.1 and illustrated in Figure 6. This procedure excluded 8 participants and yielded a final analytic sample of $N = 39$. The 39 included participants each contributed a complete within-subject triad and constituted the final sample used for all inferential analyses.

3.2 Outcome Families

3.2.1 Adherence (PLV)

To test whether visual biofeedback improved adherence to the guided box-breathing rhythm, we compared PLV across conditions. Mean PLV was $M = 0.787$ ($SD = 0.141$) for the dark-screen control, $M = 0.836$ ($SD = 0.127$) for symmetric VR, and $M = 0.860$ ($SD = 0.094$) for asymmetric VR. The planned pooled-VR-versus-dark-screen-control contrast confirmed this difference, $t(38) = 3.47$, $p = .001$, $d_z = 0.56$, 95% CI for the mean PLV difference $[0.026, 0.097]$. The symmetric-versus-asymmetric contrast was not significant, $t(38) = -1.13$, $p = .267$, $d_z = -0.18$. The order-adjusted mixed-effects omnibus supported a condition effect, $\chi^2(2) = 12.66$, $p = .002$. The corresponding Bayesian planned contrasts showed that the pooled-VR-versus-dark-screen-control difference was about 24.1 times more likely than no difference ($BF_{10} = 24.11$), whereas the symmetric-versus-asymmetric data were about 3.2 times more likely under a no-difference model ($BF_{01} = 3.22$).

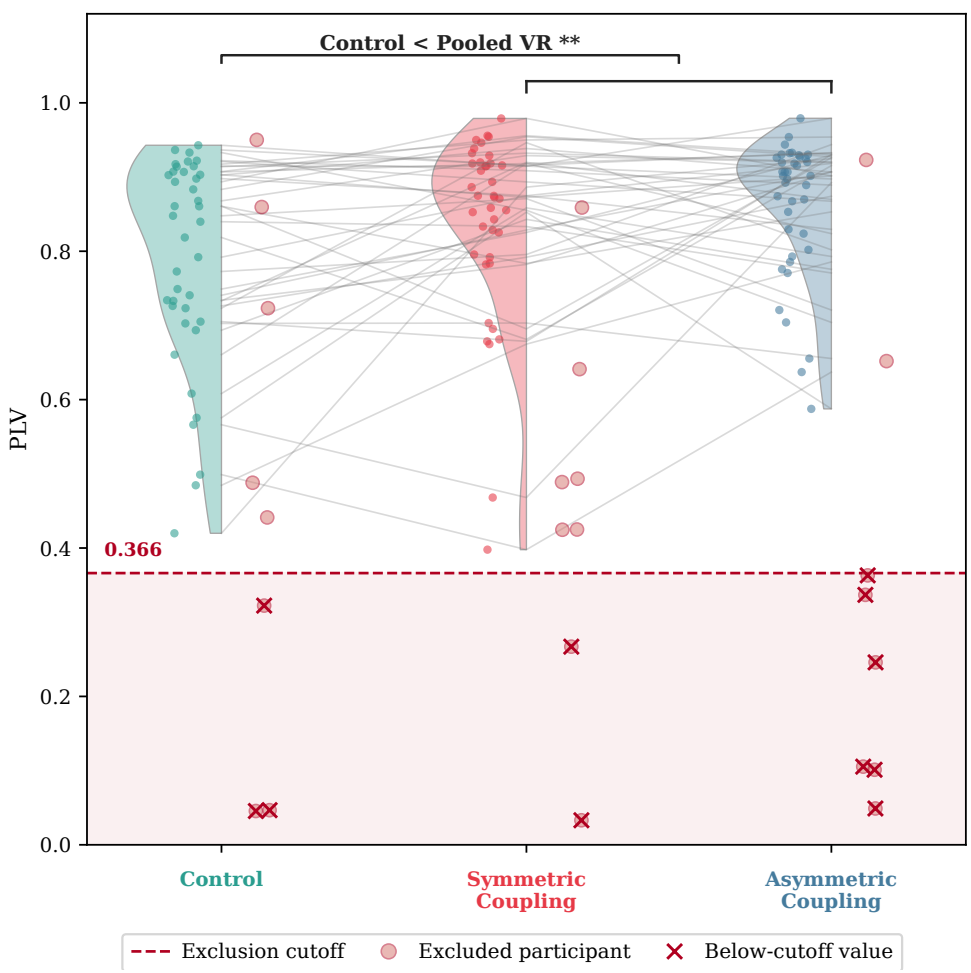


Fig. 6 Controller-derived feedback synchrony (PLV) by condition for the selected sample ($N = 39$), with condition-wise distributions and paired individual trajectories in gray. The dashed red line marks the pooled lower-tail IQR exclusion cutoff (0.366); hollow circles and red crosses indicate flagged participants and their below-cutoff values, respectively. If any single condition fell below the cutoff, the participant was excluded entirely from all analyses across all conditions

3.2.2 Self-Related Measures

To assess whether the breath-responsive virtual environment shifted subjective self-representation, we compared three pictographic measures across conditions. Only the spatial frame-of-reference continuum showed a condition effect. Participants reported a more spatially extended sense of self during virtual-reality conditions, with $M = 3.15$ ($SD = 1.41$) for the dark-screen control, $M = 4.18$ ($SD = 1.82$) for symmetric VR, and $M = 4.26$ ($SD = 1.73$) for asymmetric VR. The planned pooled-VR-versus-dark-screen-control contrast confirmed the effect, $t(38) = 4.28$, $p < .001$, $d_z = 0.69$, 95% CI $[0.56, 1.57]$. The symmetric-versus-asymmetric contrast was not

significant, $t(38) = -0.32$, $p = .752$. The registered order-adjusted omnibus result is $F(2, 75) = 10.99$, $p < .001$, $q_{\text{FDR}} < .001$, $\eta_p^2 = .227$. Neither perceived body-boundary salience ($t(38) = -0.17$, $p = .864$) nor small self ($t(38) = 1.39$, $p = .173$) showed a significant VR-versus-dark-screen-control contrast, and no self-related measure showed a significant symmetric-versus-asymmetric contrast. Figure 7 shows the response formats together with the condition-wise distributions and paired participant trajectories. Online Resource 1, Section S4 provides the complete registered frequentist and Bayesian condition-analysis inventory for all three pictographic measures.

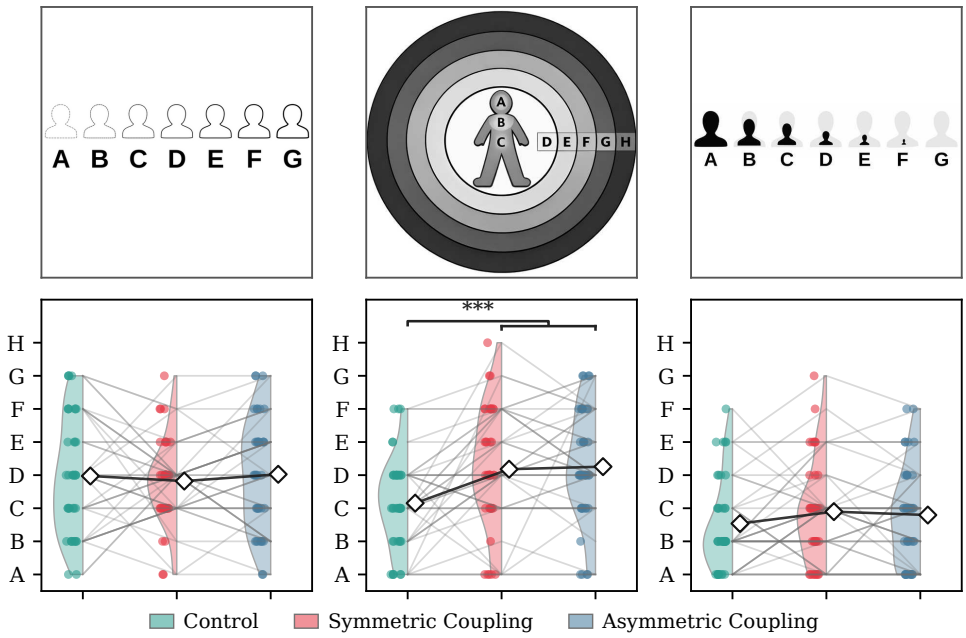


Fig. 7 Condition-wise distributions for the three pictographic self-related measures ($N = 39$). The upper row shows the administered response formats, and the lower row shows condition-wise distributions, paired participant trajectories, and means (diamonds), from left to right: Perceived Body Boundaries, the Spatial Frame of Reference Continuum (SFoRC), and Small Self. Perceived Body Boundaries is displayed in its administered A–G direction, from diffuse to sharply delineated, so higher scores indicate stronger boundary salience. Only SFoRC showed a reliable pooled-VR-versus-dark-screen-control difference. Perceived Body Boundaries and Small Self showed no reliable pooled-VR-versus-dark-screen-control differences, and no pictographic measure differed reliably between the symmetric and asymmetric VR conditions. Colors indicate the dark-screen control, symmetric VR, and asymmetric VR. The SVG pictographs in the upper row were generated in December 2025 with OpenAI Codex using GPT-5.2-Codex, based on author instructions and the published pictographs from the Perceived Body Boundaries Scale (Dambrun 2016), the Spatial Frame of Reference Continuum (Hanley et al. 2020), and the Small Self item (Vidal et al. 2025); the authors reviewed the resulting SVG files

Bayesian comparisons agreed with this pattern at the planned-contrast level. For spatial frame of reference, the observed data were approximately 204 times more likely under a pooled-VR-versus-dark-screen-control difference model than under the

no-difference model ($BF_{10} = 204.44$). Perceived body boundaries favored the no-difference model ($BF_{01} = 5.71$), whereas the Small Self result provided only weak and inconclusive evidence in the null direction ($BF_{01} = 2.39$).

Exploratory pictograph–ASC change-score analyses are reported in Online Resource 1, Section S4. Their clearest pattern was coordinated participant-level variation between spatial self-extension and positive or unity-related experience, but these post hoc associations do not alter the primary condition-effect conclusions.

3.2.3 Altered States of Consciousness

We report the altered-state family in the main text using the 3D-ASCr composites as a dimensionality-reduced summary. Online Resource 1, Section S3 reports the complete preregistered 11D-ASC analyses. The clearest pattern is stronger positive and perceptual VR-related effects, with a weaker distress-related component and no reliable symmetric-versus-asymmetric difference.

3D-ASCr composites.

Summarizing the 11D-ASC data through the 3D-ASCr composites (see Section 2.4.3 for derivation), the three higher-order dimensions showed the following pattern. Perceptual Effects had $M = 11.41$ ($SD = 12.61$) in the dark-screen control, $M = 27.25$ ($SD = 19.92$) in symmetric VR, and $M = 25.59$ ($SD = 17.24$) in asymmetric VR. Positive Effects had $M = 18.88$ ($SD = 15.39$) in the dark-screen control, $M = 25.64$ ($SD = 19.48$) in symmetric VR, and $M = 26.46$ ($SD = 17.84$) in asymmetric VR. Distressing Effects had $M = 12.33$ ($SD = 10.26$) in the dark-screen control, $M = 17.33$ ($SD = 12.66$) in symmetric VR, and $M = 17.02$ ($SD = 13.18$) in asymmetric VR. All three composites showed significant pooled-VR-versus-dark-screen-control planned contrasts: Perceptual Effects $t(38) = 4.90$, $p < .001$, $d_z = 0.79$; Positive Effects $t(38) = 3.22$, $p = .003$, $d_z = 0.51$; Distressing Effects $t(38) = 2.56$, $p = .014$, $d_z = 0.41$. Expressed on the native 0–100 scale, pooled VR increased Perceptual Effects by 15.0 points, Positive Effects by 7.2 points, and Distressing Effects by 4.8 points. These corresponded to a large effect for Perceptual Effects, a moderate effect for Positive Effects, and a smaller effect for Distressing Effects, with 76.9%, 69.2%, and 76.9% of participants, respectively, scoring higher in VR than in the dark-screen control.

No composite showed a symmetric-versus-asymmetric difference (all $p \geq .357$). The registered order-adjusted omnibus results are $F(2, 75) = 19.63$, $p < .001$, $q_{\mathrm{FDR}} < .001$, $\eta_p^2 = .344$ for Perceptual Effects; $F(2, 75) = 7.56$, $p = .001$, $q_{\mathrm{FDR}} = .002$, $\eta_p^2 = .168$ for Positive Effects; and $F(2, 75) = 4.64$, $p = .013$, $q_{\mathrm{FDR}} = .013$, $\eta_p^2 = .110$ for Distressing Effects. Bayesian omnibus comparisons favored condition models for Perceptual Effects ($BF_{10} = 121{,}810$), Positive Effects ($BF_{10} = 30.49$), and, more modestly, Distressing Effects ($BF_{10} = 3.45$). The planned Bayesian contrasts showed the same hierarchy. For pooled VR versus control, the observed data were approximately 1,178 times more likely under a difference model for Perceptual Effects ($BF_{10} = 1{,}178.41$), 13 times more likely for Positive Effects ($BF_{10} = 12.96$), and only 3 times more likely for Distressing Effects ($BF_{10} = 3.02$). For symmetric versus asymmetric VR, the observed data favored the no-difference models by factors of approximately 3.9, 5.1, and 5.7, respectively ($BF_{01} = 3.87$, 5.07, and 5.66; Figure 8). Thus, the Perceptual and Positive

pooled-VR effects had clear relative support, whereas the smaller Distressing effect had only modest Bayesian support.

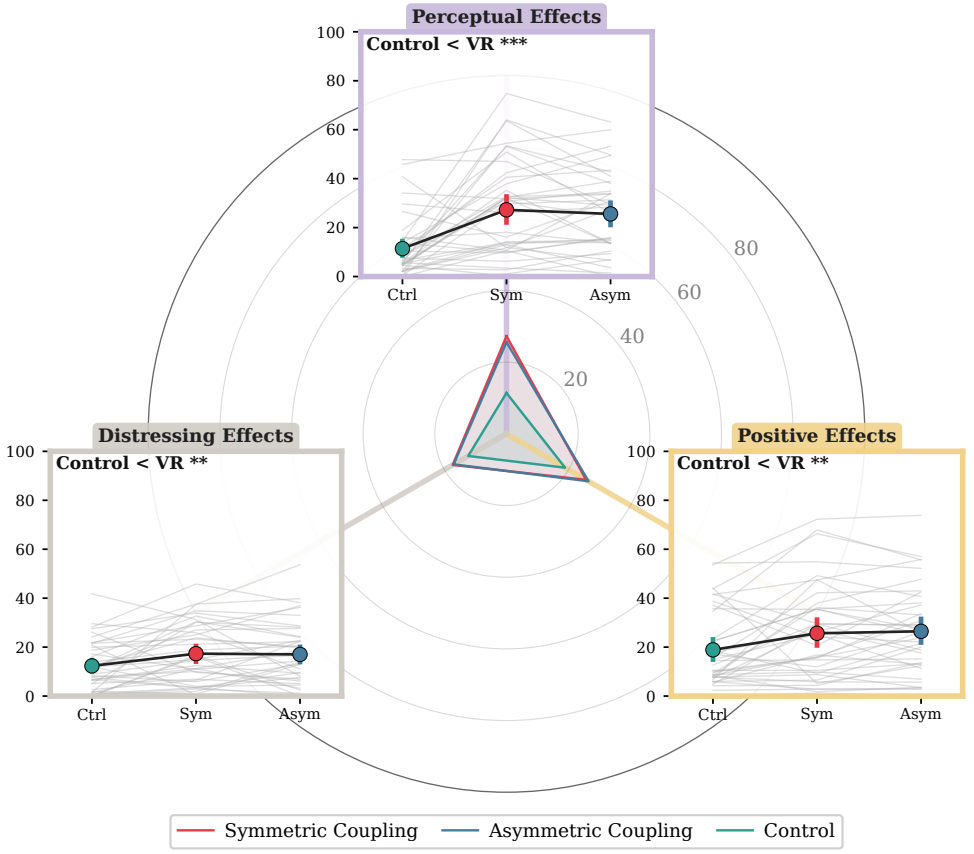


Fig. 8 Condition-wise distributions for the three 3D-ASCr composites (N = 39). All three dimensions increased in VR relative to the dark-screen control, with the largest effect for Perceptual Effects; no symmetric-versus-asymmetric differences emerged

11D-ASC questionnaire.

Complete condition descriptives and preregistered frequentist and Bayesian results for all 11 lower-order ASC dimensions, including the registered directional hypotheses, are reported in Online Resource 1, Section S3.

3.2.4 Blinding Questionnaire

Pre-unmasking responses showed selective but incomplete sensitivity to the symmetry manipulation. Mean symmetry-item accuracy was 44.2%, equivalent to approximately 1.77 of four items, and exceeded the 25% chance baseline (FDR-adjusted $q < .001$). Neutral-item accuracy was 27.6% ($q = .610$), and sham-item accuracy was 32.7%

($q = .100$); neither was clearly above chance. Across all 12 items, mean accuracy was 34.8% ($q < .001$). Participants therefore detected some genuine symmetry features, but performance remained well below perfect identification.

Post-unmasking guesses were nearly balanced: 17 participants guessed correctly (43.6%), 19 guessed incorrectly (48.7%), and 3 were uncertain (7.7%). The standard Bang blinding index was close to zero (BBI = $-.051$, 95% bootstrap CI $[-.359, .256]$). Confidence weighting changed little: the exploratory confidence-weighted index was $-.016$ (95% bootstrap CI $[-.203, .168]$, $n = 35$ directional responses). Both intervals crossed zero, indicating no reliable tendency toward either correct or opposite identification. However, the standard BBI interval extended beyond the predefined $[-0.2, 0.2]$ blinding region. The results were therefore consistent with effective blinding but too uncertain to rule out meaningful identification in either direction.

To test whether pre-unmasking sensitivity predicted subsequent condition identification, we related the 0–4 symmetry score to final-guess correctness, classified as correct versus incorrect or uncertain. Pre-unmasking symmetry-detection accuracy was descriptively higher among participants who subsequently identified the correct condition (2.00 versus 1.59 of four items), but the association was small and inconclusive (point-biserial $r = .18$, exact two-sided permutation $p = .33$; Figure 9d). Thus, better masked detection did not reliably predict the final condition guess in this sample.

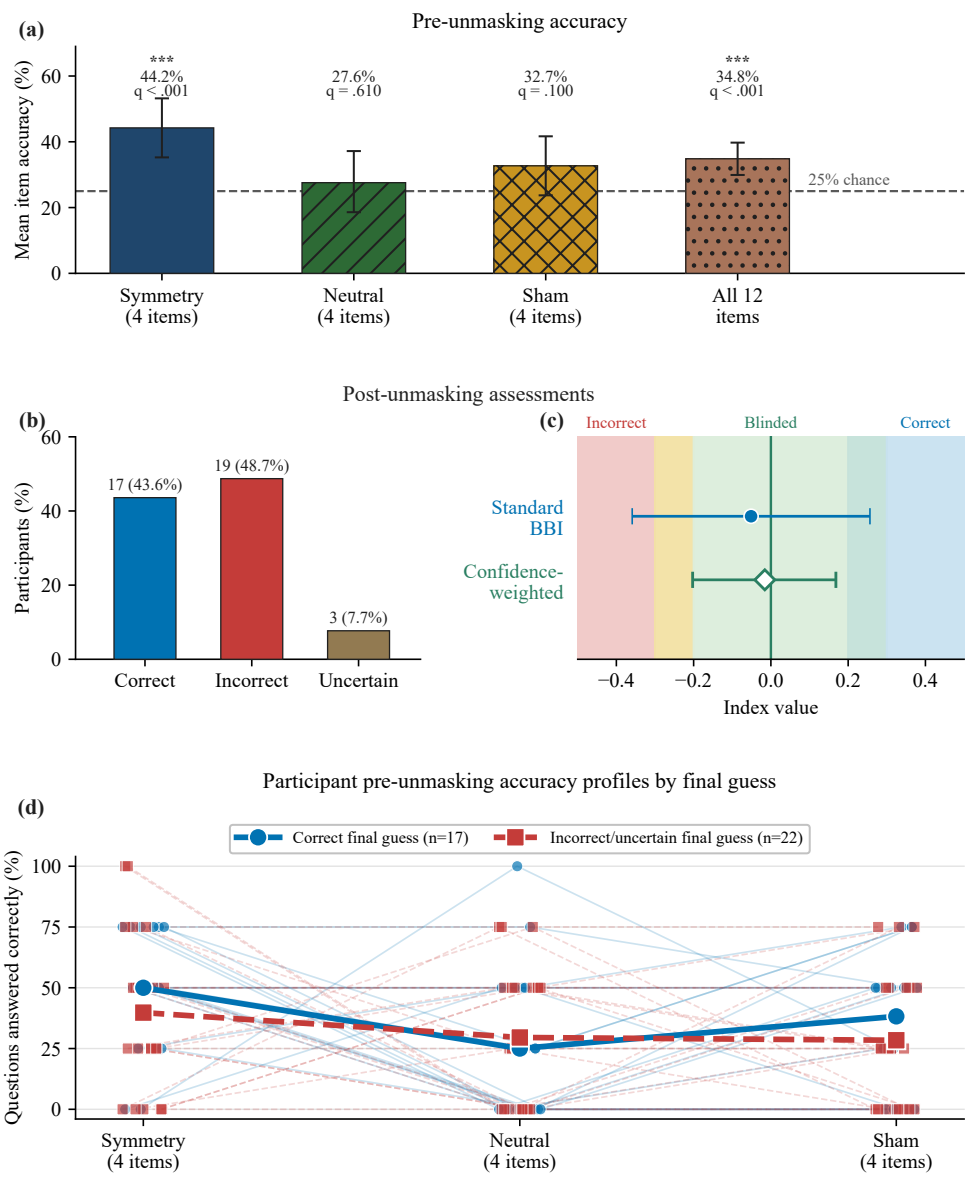


Fig. 9 Blinding and manipulation-awareness summary ($N = 39$). (a) Mean pre-unmasking accuracy for the four symmetry, four neutral, and four sham items and across all 12 items. The dashed line marks the 25% chance baseline; asterisks denote FDR-adjusted $q < .001$. (b) Post-unmasking guesses: 17 correct, 19 incorrect, and 3 uncertain. (c) Standard Bang blinding index (filled blue circle) and exploratory confidence-weighted directional index (open green diamond), with participant-bootstrap 95% confidence intervals. The shaded regions indicate incorrect, blinded, and correct identification and apply only to the standard Bang index. (d) Participant-level pre-unmasking accuracy across the three four-item categories, grouped by final-guess correctness. Thin lines and small markers represent participants; heavier lines and larger markers represent group means. Incorrect and uncertain guesses are combined

3.3 Exploratory Checks

Exploratory mixed-model checks for order and PLV moderation are reported in the OSF repository. No FDR-corrected order main effects, condition × order, condition × PLV, or condition × order × PLV interactions emerged for any ASC, 3D-ASCr, or self-related outcome family. For PLV itself, there was a main effect of order, $\chi^2(1) = 8.28$, $p = .004$, but no condition × order interaction, $\chi^2(2) = 0.37$, $p = .833$, indicating that block order did not change the between-condition adherence pattern. A planned linear contrast across session position was significant, $t(38) = -3.16$, $p = .003$, 95% CI $[-0.100, -0.022]$, indicating that PLV decreased rather than increased across sessions and therefore aligning more with waning engagement or fatigue than with a practice-improves account.

4 Discussion

This study provided a first controlled empirical evaluation of Viscereality with naive participants. Relative to audio-guided box breathing in the dark-screen control, the two VR conditions improved breathing adherence, shifted spatial self-experience toward a more expanded frame of reference, and produced an altered-state profile in which perceptual and positive effects outweighed mild distressing effects. None of the 47 tested participants discontinued the experiment because of discomfort or inability to tolerate the VR exposure. However, the preregistered aesthetic manipulation that varied the symmetry of the particle dynamics did not reliably differentiate the two active VR conditions. Taken together, these findings indicate that the paradigm produced a structured experiential profile during a brief breathing session with naive participants, but stronger control comparisons and objective measures are needed to determine the specificity and depth of these effects.

4.1 Breathing adherence and self-related experience

Participants in both active VR conditions followed the instructed breathing pattern more closely than in the dark-screen control. The display responded to participants' ongoing breathing rather than to the audio guide, so it made respiration continuously visible without telling participants how well they were matching the instructed pacing. One plausible interpretation is that the breath-responsive environment helped adherence by keeping participants engaged and by giving them the sense that their breathing was producing the visual experience. Previous findings are consistent with this. Breath-coupled VR feedback has been linked to improved focus on breathing and greater diaphragmatic movement (Blum et al. 2020; Rockstroh et al. 2021), greater focused attention and less distraction than non-VR biofeedback (Rockstroh et al. 2019), and increased interoceptive sensibility (Goral et al. 2024). A simpler explanation also remains possible. Guided breathing in the dark-screen control is presumably less engaging than the same task in an immersive environment, and the adherence metric itself was derived from how closely breathing matched the trajectory expressed by the visual display. The study would have benefited from a more stringent control, such as a visually matched scene that does not respond to breathing or one that replays

a prerecorded animation, because the engaging visual environment on its own may have contributed to the effect. This caveat matters because controlled comparisons in the VR breathing literature have not consistently shown VR-based interventions to outperform matched non-VR approaches on clinical outcomes (Cortez-Vázquez et al. 2024; Pancini et al. 2025). The present adherence finding should therefore be treated as preliminary until tested against a more stringent control.

Of the three self-related measures, only the spatial frame-of-reference continuum showed a condition effect. We had reason to expect body-boundary salience to shift as well because prior work reports reduced perceived boundary salience during meditation (Dambrun 2016); in one study that administered both scales, mindfulness training reduced perceived body boundaries and expanded allocentric spatial framing in tandem, with the boundary change mediating the spatial shift (Hanley et al. 2020). That pattern did not emerge here, perhaps because the two constructs respond to partly different triggers. Body-boundary dissolution appears to shift most reliably during practices that direct sustained attention toward the body itself, such as body-scan meditation (Dambrun 2016), mindfulness training (Hanley et al. 2020), and floatation-REST (Hruby et al. 2024). Spatial frame of reference, by contrast, has been linked not only to body-directed contemplative practice (Hanley et al. 2020) but also to perceived expansion of the physical frame of reference beyond the body (Dambrun 2023). Because Viscereality acts on the surrounding visual-spatial environment rather than directing attention toward the body, it may have engaged the spatial-frame construct through this environmental route without producing the body-focused conditions under which boundary dissolution typically occurs. Of the three scales, spatial frame of reference is also the one most closely aligned with the broader question motivating this research programme, namely whether breath-coupled changes in surrounding space can alter the felt extension of self into the environment. Previous work has shown that mapping respiration onto an externalized virtual avatar can modulate body ownership (Monti et al. 2020) and self-location (Adler et al. 2014; Betka et al. 2020) through afferent respiratory pathways (Betka et al. 2020).

However, this result requires cautious interpretation. The concentric depiction of the SFoRC scale may have resembled the expanding and contracting particle sphere shown in VR, which raises the possibility that participants selected more spatially expansive depictions because the scale imagery matched what they had just seen rather than because their felt self-boundary had shifted. This demand-characteristics concern cannot be ruled out with pictographic self-report alone and represents a clear limitation of the present measurement approach. The finding should accordingly be treated as preliminary pending corroboration from measures that do not share visual features with the stimulus, such as peripersonal space tasks. If confirmed by such measures, the spatial-frame shift would support continued investigation of whether mapping respiration onto surrounding space can modulate the felt extension of self into the environment.

Within the context of a 10-minute box-breathing exercise with ambient background music, *Viscereality* increased all three higher-order dimensions of the Altered States of Consciousness Rating Scale relative to the dark-screen control, which provided only a central fixation marker and minimal visual breathing-performance feedback.

Perceptual Effects showed the largest increase, Positive Effects a moderate increase, and Distressing Effects a smaller increase. None differed reliably between the two VR mappings that manipulated visual symmetry, and participants showed only limited feature-level sensitivity to this manipulation without reliable condition-level identification.

The fine-grained subscale decomposition and item-content analysis reveal a more specific experiential profile (Online Resource 1, Section S3.4). The perceptual shift primarily concerned simple patterns, colors, lights, and flashes, together with impressions that sound changed visual shapes or colors. These elementary visual phenomena closely matched features supplied directly by the particle environment, so their increase partly reflects overlap between the intervention and the questionnaire criteria. Participants also attributed visual changes to sound even though the same background music was presented in every condition and did not control the display. One plausible interpretation is that the richer and more dynamic visual stream provided more perceptual material that could be bound to, or retrospectively attributed to, concurrent sound, rather than producing audio-visual synaesthesia in the stricter sense. A similar distinction has been raised in psychedelic research, where LSD increased spontaneous synaesthesia-like reports that lacked the consistency and inducer specificity associated with genuine synaesthesia (Terhune et al. 2016).

The Positive Effects increase was concentrated in items reflecting a loosening of separation between self, surroundings, and time, heightened significance and emotional salience of ordinary objects, sensations of floating or diminished bodily presence, and moments of awe.

The smaller Distressing Effects increase had the character of diffuse destabilization, encompassing reduced agency, difficulty organizing thought, isolation, unexplained apprehension, and an altered or threatening quality of the surroundings. Neither constituent distress-related subscale remained reliable after correction across the fine-grained analyses. We therefore interpret the composite increase as an accumulation of mild and compatible unpleasant experiences rather than as a pronounced or clearly localized adverse response.

Descriptively, the pooled-VR ASC profile was compared with five breathwork datasets: conscious connected breathing (Bahi et al. 2024), the 90-minute breathwork arm of Airways to Alteration (Fincham et al. 2026), facilitated circular breathwork (Havenith et al. 2025), high-ventilation breathwork with music in an MRI/laboratory setting (Kartar et al. 2025), and Holotropic Breathwork (Uthaug et al. 2021). The Viscereality profile fell within the range of several of these longer breathwork datasets and showed comparatively lower distress than facilitated circular breathwork. Differences in breathing technique, duration, sample, music, facilitation, setting, and control structure make this comparison contextual rather than evidence of equivalence. Figure 10 shows the full profile overlay, and Online Resource 1, Section S3 retains the fine-grained subscale commentary.

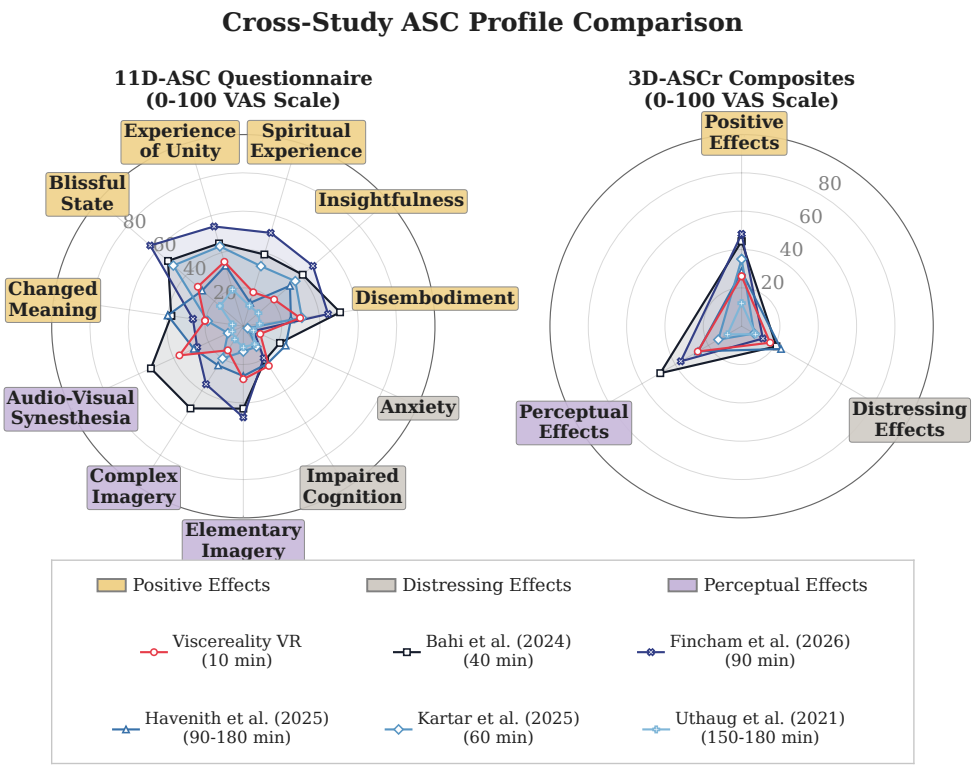


Fig. 10 Descriptive cross-study comparison of the present dataset with five named breathwork datasets. The left panel shows 11D-ASC subscale means and the right panel shows 3D-ASCr composite means. The Viscereality profile pools the symmetric and asymmetric VR conditions. Lines show raw 0–100 profile means, not standardized effect sizes; differences in technique, duration, sample, music, facilitation, and study design preclude inferential comparison. Legend order is purely graphical and does not imply a numbered study sequence

At subscale level, the profiles differed most in Experience of Unity, Spiritual Experience, Blissful State, Disembodiment, Insightfulness, and Changed Meaning of Percepts. Changed Meaning of Percepts increased in pooled VR relative to the dark-screen control in the present study, whereas Insightfulness did not change reliably. Because the reference studies differ on multiple procedural and contextual dimensions, these profile differences do not identify the mechanism responsible for any between-study contrast.

The blinding results distinguish masked feature-level sensitivity from post-unmasking condition identification. Before unmasking, symmetry-item accuracy exceeded chance, while neutral and sham accuracy did not. Participants therefore detected some genuine symmetry features, but only imperfectly. After unmasking, correct and incorrect guesses were nearly balanced, and both blinding indices were close to zero. Correct guessers had descriptively higher symmetry accuracy than incorrect or uncertain guessers, but the association was small and inconclusive ($r = .18$, exact

$p = .33$). Overall, the results were consistent with effective blinding, but the wide standard BBI interval prevented a conclusive determination.

Participants did not reliably identify the symmetric condition. Although this is consistent with blinding, it may also limit the test of the symmetry hypothesis, because explicit attention to and awareness of the manipulated feature may be necessary for it to influence emotional experience. Symmetric coherence appeared only during the breath-hold phases, approximately half of each breathing cycle, and remained secondary to the more salient breath-coupled expansion and contraction. The null difference therefore does not distinguish between an absence of an affective effect and insufficient focused exposure or awareness. We therefore plan a follow-up study that makes symmetry or particle coherence the focal stimulus dimension, manipulates it in isolation under controlled exposure, verifies that participants perceive the difference, and assesses its effects on emotional valence using physiological markers alongside direct ratings rather than relying only on retrospective altered-state ratings.

4.2 Limitations

Except for breathing-adherence PLV, the study's outcomes relied on retrospective reports completed after each condition. Such reports provide access to subjective experience but remain sensitive to recall, item wording, language, cultural context, construct coverage, and assumptions embedded in the instrument. Critiques of mystical-experience measures, for example, highlight how religious framing can shape the dimensions they assess (Sanders and Zijlmans 2021; Hovmand et al. 2023; de Deus Pontual et al. 2023). We nevertheless chose the 11D-ASC because it belongs to a widely used questionnaire family developed for standardized comparisons of altered-state phenomenology across induction methods, a role reflected in the Altered States Database (Dittrich 1998; Schmidt and Berkemeyer 2018; Prugger et al. 2022). The findings therefore remain limited by the established pitfalls of retrospective reporting, and future studies should complement psychometric assessments with concurrent physiological measures.

A concrete example is the Perceptual Effects composite, which showed the largest condition effect but was driven primarily by Elementary Imagery and Audio-Visual Synesthesia items that closely matched the visually rich particle environment. This correspondence limits the composite as standalone evidence of altered-state induction. At the same time, reports attributing visual changes to sound suggest that rich visual input may encourage retrospective cross-modal attribution, paralleling reports in psychedelic research of synaesthesia-like experiences that lack the consistency and inducer specificity of genuine synaesthesia (Terhune et al. 2016). The 11D-ASC nevertheless provides standardized cross-study context, including comparison with breathwork conducted using eye masks (Fincham et al. 2026), although such descriptive comparisons do not establish equivalence. A related concern applies to the spatial frame-of-reference result because the scale imagery resembled the intervention; our ongoing follow-up therefore combines Viscereality with an audio-tactile peripersonal-space paradigm, separating the visually presented intervention from an outcome measure that assesses spatial self-extension without relying on the visual modality.

4.3 Future directions

Future studies should test whether the altered-state effects observed in this VR setting converge across retrospective ratings and concurrent neural, autonomic, and behavioural measures. EEG complexity measures associated with breathwork phenomenology (Lewis-Healey et al. 2024), the perturbational complexity index developed to distinguish levels of consciousness (Casali et al. 2013), and heart-rate entropy examined in psychedelic states (Rosas et al. 2023) could complement 11D-ASC ratings without treating any single physiological signal as a direct readout of subjective experience. No-report paradigms could further reduce report-related confounds, although first-person validation remains necessary (Tsuchiya et al. 2015; Laukkonen and Slagter 2021). Of particular relevance to the present spatial-extension finding, an EEG-based peripersonal-space index derived from passive audio-tactile stimulation has been shown to index states of consciousness in patients with coma and related disorders of consciousness (Bertoni et al. 2026). Because spatial self-extension was assessed here by self-report, adapting such a language-independent measure could test whether those ratings converge with changes in the neural representation of peripersonal space.

Viscereality was designed to test whether breath-coupled changes in surrounding space can alter the felt boundary between self and environment. The spatial frame-of-reference finding provides preliminary support for this possibility, but a peripersonal-space task would offer a more direct behavioural test. Peripersonal space represents the multisensory boundary surrounding the body and can be estimated from response changes as stimuli approach or recede (Serino 2019; Bufacchi and Iannetti 2018; Karakoc et al. 2025).

A visuotactile peripersonal-space task could be administered during the 4-second breath holds without reusing the intervention's visual features. Comparing responses after inhalation and exhalation would test whether respiratory expansion and contraction are accompanied by corresponding changes in the represented boundary around the body. A reversed-mapping condition could then test whether any shift depends on congruence between respiratory phase and spatial direction.

We view dynamic particle systems as a potential medium for constructing abstract representations of affect in three-dimensional space. This proposal builds on evidence that affective meaning can be communicated through simple perceptual features and abstract expressions, including motion-based features (Collier 1996; de Rooij et al. 2013; Khatin-Zadeh et al. 2019) and expressive synchronization patterns of collective motion (Dietz et al. 2017; St-Onge et al. 2019; Santos and Egerstedt 2021). The present symmetry manipulation tested one aspect of this design space by varying oscillator coupling, but it produced no observable effects. This result does not exhaust the broader possibility that particle motion, spatial organization, and synchrony may map onto perceived or induced affect. Future studies should therefore examine these properties individually and in controlled combinations within a simpler valence-arousal framework, distinguishing how a display is perceived from whether it changes the user's emotional state. Short aesthetic-judgment and emotion-induction tasks could test mappings among trajectory smoothness, speed, synchronization, spatial coherence, and valence or arousal before embedding them in prolonged biofeedback sessions (Dietz et al. 2017; Santos and Egerstedt 2021). Such principle-focused testing would

provide a clearer basis for determining whether three-dimensional particle fields can communicate affective states, support their induction, or eventually encode biosignals within affect-oriented biofeedback.

The present study found that the particle system was associated with higher Positive and Perceptual Effects during box breathing, alongside a smaller Distressing Effects increase. The cross-study profile provides descriptive context only and does not establish equivalence, superior tolerability, or clinical benefit. Because the system is self-administered and the session lasted 10 minutes, future studies could test whether it supports breathing practice in settings where access to a facilitator is limited or time is scarce. High-ventilation techniques are contraindicated for individuals vulnerable to panic, syncope, or hypocapnia (Fincham et al. 2023), and a slow-paced breath-coupled VR system offers a lower-intensity entry point into breathing as a therapeutic modality.

One possible population for such testing is stroke patients, given that respiratory dysfunction and sleep-disordered breathing are common after stroke and associated with poorer recovery (Patrizz et al. 2023; Seiler et al. 2019), while structured respiratory rehabilitation remains underemphasized in clinical practice (Menezes et al. 2016). Slow-paced breathing exercises are already used to retrain respiratory function after stroke (Abdullahi et al. 2024; Yoon et al. 2022), and coupling breathing to an intuitive visual mapping of respiratory depth could engage an additional learning pathway that supports recovery of motor control over respiration. These remain illustrative possibilities. The present sample consisted of a homogeneous group of university psychology students, and testing usability, tolerability, and efficacy in clinical populations is a necessary next step.

An exploratory study of high-ventilation conscious-connected breathwork reported higher heart-rate variability immediately after the session than before it, with individual differences in this change associated with subjective experience (Canello et al. 2026). Future studies should test whether a similar pattern emerges during slow-paced breathing with immersive biofeedback.

5 Conclusion

During a brief self-administered box-breathing session, Viscereality was associated with closer synchronization to the instructed rhythm, a more spatially extended self-rating, and higher Positive, Perceptual, and smaller Distressing Effects than the dark-screen control. No measured outcome differed reliably between the symmetric and asymmetric VR mappings. These results come from a recruitment-naive university sample and do not establish equivalence to longer facilitator-supported breathwork or clinical efficacy.

Supplementary Information

Online Resource 1: Supplementary methods and analyses, including deviations from preregistration, phase-locking value computation and quality screening, complete 11D-ASC results, exploratory pictograph–ASC correspondence, temporal experience tracer analyses, and reproducibility information.

Statements and Declarations

Funding: The study reported here was funded by the BIAL Foundation through Grant 308/22, "Altered States of Viscereality: Augmenting Breathwork with Bio-Responsive Virtual Reality," awarded under the 2022 Grants Programme for Scientific Research. Continued development of Viscereality received support from the Baden-Württemberg Stiftung through the Forschungswerkstatt – Deine Idee für Morgen programme for the project "Atemräume: Integration atem- und herzratenbasierter Interaktionen in therapeutische VR-Umgebungen."

Competing interests: The authors declare no competing interests.

Ethics approval: The Ethics Committee of the University of Konstanz approved the study, which was conducted in accordance with the Declaration of Helsinki.

Consent to participate: All participants provided informed consent before participation.

Consent for publication: All participants provided written informed consent for publication and for public sharing of pseudonymized study data, as approved by the Ethics Committee of the University of Konstanz.

Availability of data and materials: Pseudonymized participant-level data, the original preregistration record, statistical analysis outputs, figure-generation scripts, study materials, and reproducibility documentation are available in the versioned reproducibility package (Fejer et al. 2026b); a mirror is available at OSF: https://doi.org/10.17605/OSF.IO/64MWK.

Code availability: The statistical analysis and figure-generation scripts, exact environment specifications, and replay instructions are included in the same versioned reproducibility package (Fejer et al. 2026b).

Authors' contributions: George Fejer: Conceptualization, Data curation, Formal analysis, Funding acquisition, Investigation, Methodology, Project administration, Software, Validation, Visualization, Writing – original draft, Writing – review & editing. Till Holzapfel: Conceptualization, Methodology, Resources, Software, Validation, Visualization. Taru Hirvonen: Methodology, Resources, Software, Visualization. Anestis Lalidis Mateo: Methodology, Resources, Software, Validation. Johannes Blum: Methodology, Resources, Software, Validation. Michael Gaebler: Conceptualization, Project administration, Supervision, Writing – review & editing. Bigna Lenggenhager: Conceptualization, Funding acquisition, Supervision, Writing – review & editing.

References

Abdullahi A, Wong TWL, Ng SSM (2024) Efficacy of diaphragmatic breathing exercise on respiratory, cognitive, and motor function outcomes in patients with stroke: a systematic review and meta-analysis. Frontiers in Neurology 14:1233408. https://doi.org/10.3389/fneur.2023.1233408, URL https://doi.org/10.3389/fneur.2023.1233408

Acebrón JA, Bonilla LL, Pérez Vicente CJ, et al (2005) The kuramoto model: A simple paradigm for synchronization phenomena. Reviews of modern physics 77(1):137–185. https://doi.org/10.1103/RevModPhys.77.137

Adler D, Herbelin B, Similowski T, et al (2014) Breathing and sense of self: Visuo-respiratory conflicts alter body self-consciousness. Respiratory Physiology & Neurobiology 203:68–74. https://doi.org/10.1016/j.resp.2014.08.003, URL https://doi.org/10.1016/j.resp.2014.08.003

Ashhad S, Kam K, Del Negro CA, et al (2022) Breathing rhythm and pattern and their influence on emotion. Annual Review of Neuroscience 45:223–247. https://doi.org/10.1146/annurev-neuro-090121-014424

Aspell JE, Heydrich L, Marillier G, et al (2013) Turning body and self inside out. Psychological Science 24(12):2445–2453. https://doi.org/10.1177/0956797613498395, URL https://doi.org/10.1177/0956797613498395

Baertsch N, Reily E, Sedano J, et al (2025) Multimodal breathing control: Pontomedullary mechanisms and current perspectives. BioEssays 47:e70072. https://doi.org/10.1002/bies.70072

Bahi C, Irrmischer M, Franken K, et al (2024) Effects of conscious connected breathing on cortical brain activity, mood and state of consciousness in healthy adults. Current Psychology 43(12):10578–10589. https://doi.org/10.1007/s12144-023-05119-6

Bang H, Ni L, Davis CE (2004) Assessment of blinding in clinical trials. Controlled Clinical Trials 25(2):143–156. https://doi.org/10.1016/j.cct.2003.10.016

Bentley TJC, Mitchell L, Sutton S (2023) Breathing interventions for stress: A systematic review and meta-analysis. International Journal of Mental Health Promotion 25(3):357–381

Bertamini M, Makin ADJ, Rampone G (2013) Implicit association of symmetry with positive valence, high arousal and simplicity. i-Perception 4(5):317–327. https://doi.org/10.1068/i0601jw

Bertoni T, Ricci G, Jöhr J, et al (2026) Multisensory integration in peripersonal space indexes consciousness states in sleep and disorders of consciousness. Cell Reports Medicine 7(4):102705. https://doi.org/10.1016/j.xcrm.2026.102705, URL https://doi.org/10.1016/j.xcrm.2026.102705

Betka S, Canzoneri E, Adler D, et al (2020) Mechanisms of the breathing contribution to bodily self-consciousness in healthy humans: Lessons from machine-assisted breathing? Psychophysiology 57(8):e13564. https://doi.org/10.1111/psyp.13564, URL https://doi.org/10.1111/psyp.13564

Blum J, Rockstroh C, Göritz AS (2019) Heart rate variability biofeedback based on slow-paced breathing with immersive virtual reality nature scenery. Frontiers in psychology 10:2172. https://doi.org/10.3389/fpsyg.2019.02172

Blum J, Rockstroh C, Göritz AS (2020) Development and pilot test of a virtual reality respiratory biofeedback approach. Applied Psychophysiology and Biofeedback 45(3):153–163. https://doi.org/10.1007/s10484-020-09468-x

Boiten FA, Frijda NH, Wientjes CJE (1994) Emotions and respiratory patterns: review and critical analysis. International Journal of Psychophysiology 17(2):103–128. https://doi.org/10.1016/0167-8760(94)90027-2

Bossenbroek R, Wols A, Weerdmeester J, et al (2020) Efficacy of a virtual reality biofeedback game (DEEP) to reduce anxiety and disruptive classroom behavior: single-case study. JMIR Mental Health 7(3):e16066. https://doi.org/10.2196/16066, URL https://doi.org/10.2196/16066

Bufacchi RJ, Iannetti GD (2018) An action field theory of peripersonal space. Trends in Cognitive Sciences 22(12):1076–1090. https://doi.org/10.1016/j.tics.2018.09.004

Canello T, Tlaie A, Chalise K, et al (2026) Non-ordinary states of consciousness evoked by breathwork correlate with improved heart-rate variability. Scientific Reports https://doi.org/10.1038/s41598-026-59995-6, URL https://doi.org/10.1038/s41598-026-59995-6

Casali AG, Gosseries O, Rosanova M, et al (2013) A theoretically based index of consciousness independent of sensory processing and behavior. Science Translational Medicine 5(198):198ra105. https://doi.org/10.1126/scitranslmed.3006294

Collier GL (1996) Affective synesthesia: Extracting emotion space from simple perceptual stimuli. Motivation and Emotion 20(1):1–32. https://doi.org/10.1007/BF02251005, URL https://doi.org/10.1007/BF02251005

Corne S, Bshouty Z (2005) Basic principles of control of breathing. Respiratory Care Clinics of North America 11(2):147–172. https://doi.org/10.1016/j.rcc.2005.02.011

Cortez-Vázquez G, Adriaanse M, Burchell GL, et al (2024) Virtual reality breathing interventions for mental health: A systematic review and meta-analysis of randomized controlled trials. Applied Psychophysiology and Biofeedback 49(1):1–21. https://doi.org/10.1007/s10484-023-09611-4, URL https://doi.org/10.1007/s10484-023-09611-4

Dambrun M (2016) When the dissolution of perceived body boundaries elicits happiness: The effect of selflessness induced by a body scan meditation. Consciousness and Cognition 46:89–98. https://doi.org/10.1016/j.concog.2016.09.013

Dambrun M (2023) Beyond the body/self-consciousness matrix: Scale of the physical frame of reference and self-transcendence experience. Psychology of Consciousness: Theory, Research, and Practice 10(3):292–312. https://doi.org/10.1037/cns0000314, URL https://doi.org/10.1037/cns0000314

de Deus Pontual AA, Senhorini HG, Corradi-Webster CM, et al (2023) Systematic review of psychometric instruments used in research with psychedelics. Journal of Psychoactive Drugs 55(3):359–368. https://doi.org/10.1080/02791072.2022.2079108

Dietz G, Jane L. E., Washington P, et al (2017) Human perception of swarm robot motion. In: Proceedings of the 2017 CHI Conference Extended Abstracts on Human Factors in Computing Systems. ACM, pp 2520–2527, https://doi.org/10.1145/3027063.3053220, URL https://doi.org/10.1145/3027063.3053220

Dittrich A (1998) The standardized psychometric assessment of altered states of consciousness (ascs) in humans. Pharmacopsychiatry 31(S2):80–84. https://doi.org/10.1055/s-2007-979351

van Doorn JB, van den Bergh D, Bohm U, et al (2021) The JASP guidelines for conducting and reporting a bayesian analysis. Psychonomic Bulletin & Review 28(3):813–826. https://doi.org/10.3758/s13423-020-01798-5

Fejer G, Holzapfel T, Gómez-Emilsson A, et al (2025) Viscereality: A bio-responsive vr system for breath-based interactions and coupled oscillator dynamics to augment altered states of consciousness. In: Mensch und Computer 2025 Workshopband, Gesellschaft für Informatik e.V., https://doi.org/10.18420/muc2025-mci-ws11-174, URL https://dl.gi.de/handle/20.500.12116/46829

Fejer G, Holzapfel T, Hirvonen T, et al (2026a) Breathing space: Spatial mapping of breath and cardiac biofeedback for affective state representation and coherence training in viscereality. In: Proceedings of the 1st International Conference on Human-Computer Interaction in the Alps. ACM, pp 79–86, https://doi.org/10.1145/3780045.3780061

Fejer G, Holzapfel T, Hirvonen T, et al (2026b) Viscereality: Bioresponsive virtual reality for box breathing and altered-state experience: Study 3 reproducibility package. https://doi.org/10.5281/zenodo.22073981, URL https://doi.org/10.5281/zenodo.22073981

Fincham GW, Strauss C, Montero-Marin J, et al (2023) Effect of breathwork on stress and mental health: A meta-analysis of randomised-controlled trials. Scientific Reports 13(1):432. https://doi.org/10.1038/s41598-022-27247-y

Fincham GW, Caddye E, Kartar AA, et al (2026) An exploratory study of breathwork-induced altered states of consciousness in experienced practitioners: the airways to alteration (A2A) trial. Frontiers in Psychology 17:1851882. https://doi.org/10.3389/fpsyg.2026.1851882

Glowacki DR (2024) VR models of death and psychedelics: An aesthetic paradigm for design beyond day-to-day phenomenology. Frontiers in Virtual Reality 4:1286950. https://doi.org/10.3389/frvir.2023.1286950, URL https://doi.org/10.3389/frvir.2023.1286950

Glowacki DR, Wonnacott MD, Freire R, et al (2020) Isness: Using multi-person VR to design peak mystical type experiences comparable to psychedelics. In: Proceedings of the 2020 CHI Conference on Human Factors in Computing Systems. ACM, pp 1–14, https://doi.org/10.1145/3313831.3376649, URL https://doi.org/10.1145/3313831.3376649

Glowacki DR, Williams RR, Wonnacott MD, et al (2022) Group VR experiences can produce ego attenuation and connectedness comparable to psychedelics. Scientific Reports 12(1):8995. https://doi.org/10.1038/s41598-022-12637-z, URL https://doi.org/10.1038/s41598-022-12637-z

Goral O, Wald IY, Maimon A, et al (2024) Enhancing interoceptive sensibility through exteroceptive-interoceptive sensory substitution. Scientific Reports 14(1):14855. https://doi.org/10.1038/s41598-024-63231-4, URL https://doi.org/10.1038/s41598-024-63231-4

Hanley AW, Garland EL (2019) Spatial frame of reference as a phenomenological feature of self-transcendence: Measurement and manipulation through mindfulness meditation. Psychology of Consciousness: Theory, Research, and Practice 6(4):329–345. https://doi.org/10.1037/cns0000204

Hanley AW, Dambrun M, Garland EL (2020) Effects of mindfulness meditation on self-transcendent states: Perceived body boundaries and spatial frames of reference. Mindfulness 11(5):1194–1203. https://doi.org/10.1007/s12671-020-01330-9

Havenith MN, Leidenberger M, Brasanac J, et al (2025) Decreased co2 saturation during circular breathwork supports emergence of altered states of consciousness. Communications Psychology 3(1):59. https://doi.org/10.1038/s44271-025-00247-0

Homma I, Masaoka Y (2008) Breathing rhythms and emotions. Experimental Physiology 93(9):1011–1021. https://doi.org/10.1113/expphysiol.2008.042424

Hovmand OR, Poulsen ED, Arnfred S (2023) Assessment of the acute subjective psychedelic experience: A review of patient-reported outcome measures in clinical research on classical psychedelics. Journal of Psychopharmacology 38(1):19–32. https://doi.org/10.1177/02698811231200019

Hovmand OR, Madsen M, Fisher PM, et al (2024) Altered states of consciousness in danish healthy volunteers and recreational users of psilocybin and the possible impact of setting and intention: Danish validation of the five-dimensional altered states of consciousness questionnaire. Journal of Psychopharmacology 38(9):924–932. https://doi.org/10.1177/02698811241269669

Hruby H, Schmidt S, Feinstein JS, et al (2024) Induction of altered states of consciousness during Floatation-REST is associated with the dissolution of body boundaries and the distortion of subjective time. Scientific Reports 14(1):9316. https://doi.org/10.1038/s41598-024-59642-y, URL https://doi.org/10.1038/s41598-024-59642-y

Jerath R, Beveridge C (2020) Respiratory rhythm, autonomic modulation, and the spectrum of emotions: The future of emotion recognition and modulation. Frontiers in Psychology 11:1980. https://doi.org/10.3389/fpsyg.2020.01980

Johnson ME (2023) Qualia formalism and a symmetry theory of valence. OpenTheory, URL https://opentheory.net/Qualia_Formalism_and_a_Symmetry_Theory_of_Valence.pdf

Karakoc C, Lucifora C, Massimino S, et al (2025) Extending peri-personal space in immersive virtual reality: A systematic review. Virtual Worlds 4(1):5. https://doi.org/10.3390/virtualworlds4010005, URL https://doi.org/10.3390/virtualworlds4010005

Kartar AA, Horinouchi T, Örzsik B, et al (2025) Neurobiological substrates of altered states of consciousness induced by high ventilation breathwork accompanied by music. PLOS One 20(8):e0329411. https://doi.org/10.1371/journal.pone.0329411, URL https://doi.org/10.1371/journal.pone.0329411

Khatin-Zadeh O, Eskandari Z, Vahdat S, et al (2019) Why are motions effective in describing emotions? Polish Psychological Bulletin 50(2):119–124. https://doi.org/10.24425/ppb.2019.126027

Kodithuwakku Arachchige SNK, Chander H, Freeman H, et al (2022) The walls are closing in: postural responses to a virtual reality claustrophobic simulation. Clinical and Translational Neuroscience 6(2):15. https://doi.org/10.3390/ctn6020015

Kolahi J, Bang H, Park J (2009) Towards a proposal for assessment of blinding success in clinical trials: Up-to-date review. Community Dentistry and Oral Epidemiology 37(6):477–484. https://doi.org/10.1111/j.1600-0528.2009.00494.x

Kruschke JK (2021) Bayesian analysis reporting guidelines. Nature Human Behaviour 5(10):1282–1291. https://doi.org/10.1038/s41562-021-01177-7

Laborde S, Allen MS, Borges U, et al (2022) Effects of voluntary slow breathing on heart rate and heart rate variability: a systematic review and a meta-analysis. Neuroscience & Biobehavioral Reviews 138:104711. https://doi.org/10.1016/j.neubiorev.2022.104711

Laukkonen RE, Slagter HA (2021) From many to (n)one: Meditation and the plasticity of the predictive mind. Neuroscience & Biobehavioral Reviews 128:199–217. https://doi.org/10.1016/j.neubiorev.2021.06.021

Lewis-Healey E, Tagliazucchi E, Canales-Johnson A, et al (2024) Breathwork-induced psychedelic experiences modulate neural dynamics. Cerebral Cortex 34(8):bhae347. https://doi.org/10.1093/cercor/bhae347

Makin ADJ, Wilton MM, Pecchinenda A, et al (2012) Symmetry perception and affective responses: A combined eeg/emg study. Neuropsychologia 50(14):3250–3261. https://doi.org/10.1016/j.neuropsychologia.2012.10.003

Marchant J, Khazan I, Cressman M, et al (2025) Comparing the effects of square, 4–7–8, and 6 breaths-per-minute breathing conditions on heart rate variability, CO2 levels, and mood. Applied Psychophysiology and Biofeedback 50(2):261–276. https://doi.org/10.1007/s10484-025-09688-z

McGraw KO, Wong SP (1992) A common language effect size statistic. Psychological Bulletin 111(2):361–365. https://doi.org/10.1037/0033-2909.111.2.361, URL https://doi.org/10.1037/0033-2909.111.2.361

Menezes KKP, Nascimento LR, Ada L, et al (2016) Respiratory muscle training increases respiratory muscle strength and reduces respiratory complications after stroke: a systematic review. Journal of Physiotherapy 62(3):138–144. https://doi.org/10.1016/j.jphys.2016.05.014, URL https://doi.org/10.1016/j.jphys.2016.05.014

Monti A, Porciello G, Tieri G, et al (2020) The "embreathment" illusion highlights the role of breathing in corporeal awareness. Journal of Neurophysiology 123(1):420–427. https://doi.org/10.1152/jn.00617.2019, URL https://doi.org/10.1152/jn.00617.2019

Morey RD, Rouder JN (2024) BayesFactor: Computation of Bayes Factors for Common Designs. https://doi.org/10.32614/CRAN.package.BayesFactor, URL https://CRAN.R-project.org/package=BayesFactor, r package version 0.9.12-4.7

Pancini E, Di Natale AF, Villani D (2025) Breathing in virtual reality for promoting mental health: a scoping review. Virtual Reality 29(1):29. https://doi.org/10.1007/s10055-024-01096-8, URL https://doi.org/10.1007/s10055-024-01096-8

Patrizz A, El Hamamy A, Maniskas M, et al (2023) Stroke-induced respiratory dysfunction is associated with cognitive decline. Stroke 54(7):1863–1874. https://doi.org/10.1161/STROKEAHA.122.041239, URL https://doi.org/10.1161/STROKEAHA.122.041239

Pecchinenda A, Bertamini M, Makin AD, et al (2014) The pleasantness of visual symmetry: always, never or sometimes. PLoS ONE 9(3):e92685. https://doi.org/10.1371/journal.pone.0092685

Pöhlmann KMT, Föcker J, Dickinson P, et al (2021) The effect of motion direction and eccentricity on vection, VR sickness and head movements in virtual reality. Multisensory Research 34(6):623–662. https://doi.org/10.1163/22134808-bja10049

Prpa M, Stepanova ER, Schiphorst T, et al (2020) Inhaling and exhaling: How technologies can perceptually extend our breath awareness. In: Proceedings of the 2020 CHI Conference on Human Factors in Computing Systems, pp 1–15

Prugger J, Derdiyok E, Dinkelacker J, et al (2022) The altered states database: Psychometric data from a systematic literature review. Scientific Data 9(1):720. https://doi.org/10.1038/s41597-022-01822-4

Qin Z, Yu Y, Gu H, et al (2024) Sas macro programme for Bang's Blinding Index to assess and visualise the success of blinding in randomised controlled trials. General Psychiatry 37:e101578. https://doi.org/10.1136/gpsych-2024-101578

Rockstroh C, Blum J, Göritz AS (2019) Virtual reality in the application of heart rate variability biofeedback. International Journal of Human-Computer Studies 130:209–220. https://doi.org/10.1016/j.ijhcs.2019.06.011, URL https://doi.org/10.1016/j.ijhcs.2019.06.011

Rockstroh C, Blum J, Göritz AS (2021) A mobile VR-based respiratory biofeedback game to foster diaphragmatic breathing. Virtual Reality 25(2):539–552. https://doi.org/10.1007/s10055-020-00471-5, URL https://doi.org/10.1007/s10055-020-00471-5

Rodrigues FA, Peron TKDM, Ji P, et al (2016) The kuramoto model in complex networks. Physics Reports 610:1–98. https://doi.org/10.1016/j.physrep.2015.10.008

Rogers B, Graham M (1979) Motion parallax as an independent cue for depth perception. Perception 8(2):125–134. https://doi.org/10.1068/p080125, URL https://doi.org/10.1068/p080125

de Rooij A, Broekens J, Lamers MH (2013) Abstract expressions of affect. International Journal of Synthetic Emotions 4(1):1–31. https://doi.org/10.4018/jse.2013010101, URL https://doi.org/10.4018/jse.2013010101

Rosas FE, Mediano PAM, Timmermann C, et al (2023) The entropic heart: Tracking the psychedelic state via heart rate dynamics. bioRxiv p 2023.11.07.566008. https://doi.org/10.1101/2023.11.07.566008, URL https://doi.org/10.1101/2023.11.07.566008

Sanders JW, Zijlmans J (2021) Moving past mysticism in psychedelic science. ACS Pharmacology & Translational Science 4(3):1253–1255. https://doi.org/10.1021/acsptsci.1c00097, URL https://doi.org/10.1021/acsptsci.1c00097

Santos M, Egerstedt M (2021) From motions to emotions: Can the fundamental emotions be expressed in a robot swarm? International Journal of Social Robotics 13(4):751–764. https://doi.org/10.1007/s12369-020-00665-6, URL https://doi.org/10.1007/s12369-020-00665-6

Schmidt TT, Berkemeyer H (2018) The altered states database: Psychometric data of altered states of consciousness. Frontiers in Psychology 9:1028. https://doi.org/10.3389/fpsyg.2018.01028

Schmitz CN, Bernardic M, Vlădoiu AD, et al (2026) How high ventilation breathwork alters consciousness: Hypoperfusion, network dynamics, and subjective experience. Progress in Neuropsychopharmacology & Biological Psychiatry 149:111873. https://doi.org/10.1016/j.pnpbp.2026.111873, URL https://doi.org/10.1016/j.pnpbp.2026.111873

Seiler A, Camilo M, Korostovtseva L, et al (2019) Prevalence of sleep-disordered breathing after stroke and TIA. Neurology 92(7):e648–e654. https://doi.org/10.1212/WNL.0000000000006904, URL https://doi.org/10.1212/WNL.0000000000006904

Serino A (2019) Peripersonal space (PPS) as a multisensory interface between the individual and the environment, defining the space of the self. Neuroscience & Biobehavioral Reviews 99:138–159. https://doi.org/10.1016/j.neubiorev.2019.01.016

Shi L, Liu F, Liu Y, et al (2023) Biofeedback respiratory rehabilitation training system based on virtual reality technology. Sensors 23(22):9025. https://doi.org/10.3390/s23229025, URL https://doi.org/10.3390/s23229025

St-Onge D, Levillain F, Zibetti E, et al (2019) Collective expression: How robotic swarms convey information with group motion. Paladyn, Journal of Behavioral Robotics 10(1):418–435. https://doi.org/10.1515/pjbr-2019-0033, URL https://doi.org/10.1515/pjbr-2019-0033

Stocker K, Hartmann M, Schmid Y, et al (2025) The 3d-ascr scale: A revalidation of the core dimensions of the altered states of consciousness rating scale 5d(11)-asc for psychedelic research. Journal of Psychopharmacology https://doi.org/10.1177/02698811251397328

Studerus E, Gamma A, Vollenweider FX (2010) Psychometric evaluation of the altered states of consciousness rating scale (oav). PLOS ONE 5(8):e12412. https://doi.org/10.1371/journal.pone.0012412

Suzuki K, Garfinkel SN, Critchley HD, et al (2013) Multisensory integration across exteroceptive and interoceptive domains modulates self-experience in the rubber-hand illusion. Neuropsychologia 51(13):2909–2917. https://doi.org/10.1016/j.neuropsychologia.2013.08.014

Terhune DB, Luke DP, Kaelen M, et al (2016) A placebo-controlled investigation of synaesthesia-like experiences under LSD. Neuropsychologia 88:28–34. https://doi.org/10.1016/j.neuropsychologia.2016.04.005

Tinga AM, Nyklíček I, Jansen MP, et al (2019) Respiratory biofeedback does not facilitate lowering arousal in meditation through virtual reality. Applied Psychophysiology and Biofeedback 44(1):51–59. https://doi.org/10.1007/s10484-018-9421-5, URL https://doi.org/10.1007/s10484-018-9421-5

Tsuchiya N, Wilke M, Frässle S, et al (2015) No-report paradigms: Extracting the true neural correlates of consciousness. Trends in Cognitive Sciences 19(12):757–770. https://doi.org/10.1016/j.tics.2015.10.002

Uthaug MV, Mason NL, Havenith MN, et al (2021) An experience with Holotropic Breathwork is associated with improvement in non-judgement and satisfaction with life while reducing symptoms of stress in a Czech-speaking population. Journal of Psychedelic Studies 5(3):176–189. https://doi.org/10.1556/2054.2021.00193, URL https://doi.org/10.1556/2054.2021.00193

Vicary S, Sperling M, von Zimmermann J, et al (2017) Joint action aesthetics. PLOS ONE 12(7):e0180101. https://doi.org/10.1371/journal.pone.0180101

Vidal J, Andreu CI, Wrzesien M, et al (2025) Inducing selflessness through a numadelic virtual reality experience: a preliminary study. Virtual Reality 30(1). https://doi.org/10.1007/s10055-025-01293-z, URL https://doi.org/10.1007/s10055-025-01293-z

Wald IY, Maimon A, Keniger de Andrade Gensas L, et al (2023) Breathing based immersive interactions for enhanced agency and body awareness: A claustrophobia motivated study. In: Extended Abstracts of the 2023 CHI Conference on Human Factors in Computing Systems, pp 1–7, https://doi.org/10.1145/3544549.3585897, URL https://doi.org/10.1145/3544549.3585897

Yoon JM, Im SC, Kim K (2022) Effects of diaphragmatic breathing and pursed lip breathing exercises on the pulmonary function and walking endurance in patients with chronic stroke: a randomised controlled trial. International Journal of Therapy and Rehabilitation 29(8):1–11. https://doi.org/10.12968/ijtr.2021.0027, URL https://doi.org/10.12968/ijtr.2021.0027

Zaccaro A, Piarulli A, Laurino M, et al (2018) How breath-control can change your life: a systematic review on psycho-physiological correlates of slow breathing. Frontiers in Human Neuroscience 12:353. https://doi.org/10.3389/fnhum.2018.00353

Zaccaro A, Piarulli A, Melosini L, et al (2022) Neural correlates of non-ordinary states of consciousness in pranayama practitioners: the role of slow nasal breathing. Frontiers in Systems Neuroscience 16:803904. https://doi.org/10.3389/fnsys.2022.803904

Supplementary Files

This is a list of supplementary files associated with this preprint. Click to download.

- ESM1.pdf